Molecular Mechanics Calculations of Tin-bis(triphenylphosphine oxide) Complexes

by

Andrea Dalacu

A Thesis

submitted to the Department of Chemistry

in partial fulfillment of the requirements

for the degree of

Master of Science

July 1994

Brock University

St Catharines, Ontario

ABSTRACT

The capability of molecular mechanics for modeling the wide distribution of bond angles and bond lengths characteristic of coordination complexes was investigated. This was the preliminary step for future modeling of solvent extraction. Several tin-phosphine oxide complexes were selected as the test group for the desired range of geometry they exhibited as well as the ligands they contained, which were of interest in connection with solvation. A variety of adjustments were made to Allinger's MM2 force-field in order to improve its performance in the treatment of these systems.

A set of unique force constants was introduced for those terms representing the metal ligand bond lengths, bond angles, and, torsion angles. These were significantly smaller than traditionally used with organic compounds.

The Morse potential energy function was incorporated for the M-X bond lengths and the cosine harmonic potential energy function was invoked for the MOP bond angle. These functions were found to accomodate the wide distribution of observed values better than the traditional harmonic approximations.

Crystal packing influences on the MOP angle were explored through the inclusion of the isolated molecule within a shell containing the nearest neighbors during energy minimization experiments. This was found to further improve the fit of the MOP angle.

ACKNOWLEDGEMENTS

It is my great pleasure to thank Dr. Mary Frances Richardson for the time and support she invested to make me a better researcher. I hope one day to achieve her level of knowledge, enthusiasm and wisdom.

I would like to thank Professor Ian Brindle for being a friendly face whose door was aways open and who was always helpful.

My appreciation is extended to Dr. Richard Hiatt and Dr. Jack Miller for their role as members of my committee.

I would like also to thank Tim Jones his help and for answering my incessant questions.

Joanne, without your anxiety attacks I would probably still be looking for incentive, I cannot imagine what I would have done without you here.

Matthew... well you know.

TABLE OF CONTENTS

LIST OF TABLES

LIST OF FIGURES

I. INTRODUCTION

The group of elements known as heavy metals has received a great deal of publicity in recent years. Incidents of mercury and lead poisonings have been splashed all over headlines and have very dramatically brought to our attention the toxicity of some heavy metals. The original panic initiated a large number of studies on the effects of different exposure levels to various organisms. At this time it is known that many of these elements are essential at trace levels in most life forms[1] but the effects of higher concentrations are still relatively unknown. There is substantial evidence, however, that some heavy metals are linked to cancer and some may be neurotoxins[2].

The health risks, alone, associated with this group of compounds have been sufficient to instigate cleanup measures. Compounded with responsible industrial practices, economic incentives also exist for metal retrieval. It is becoming increasingly difficult and expensive to simply find

natural sources of these materials. As a result of these two factors the rate of research in metal reclamation techniques is growing daily.

A. Solvation and solvent extraction

Adsorption, ion exchange, chemical reduction and precipitation are techniques which are currently in use for metal recovery.[3] These methods are somewhat limiting and the use of solvent extraction is being reinvestigated as a practical alternative.[4,5]

Solvent extraction relies on the behavior of a solute at the interface of two immiscible phases.[6] Extraction occurs when the solute crosses the interface and accumulates preferentially in the extract. An important factor in determining the efficiency of this transfer is the affinity of the solute for the extract, another is the surface area of the interface across which transfer can take place. By creating the appropriate set of conditions, solvent extraction can be a reliable and efficient method

for metal recovery.

The efficiency of the solute extraction may be defined in terms of a distribution coefficient, D[6]:

$$D = \frac{[M_{org}]}{[M_{aq}]} \qquad [1]$$

where $[M_{org}]$ is the concentration of metal in the organic phase and $[M_{aq}]$ is the concentration of metal in the aqueous phase.

Application of liquid-liquid extraction to recovery of metals from wastewater would require a solvent which is immiscible with water and in which the metal salt or complex is more soluble. Organic solvents are quite often immiscible with water, but the same characteristics which make them hydrophobic also make them poor solvents for metal ions. To enhance metal transfer to the organic medium, the metal may be complexed so that it acquires some of the characteristics of an organic compound. Complexation can transform the metal so that it attains

some of the properties of organic solvents such as zero net charge, low polarity and low polarizability. If the ligands are selected carefully, the complex can be designed to be very similar to any solvent. For example:

$$MO_2^{2+} + 2NO_3^- + 2[(C_4H_9O)_3PO] \longrightarrow$$

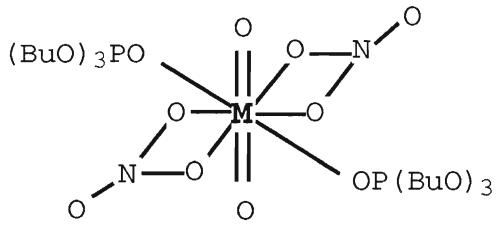

The complex formed would then be soluble in $(C_4H_9O)PO$ as well as non-polar organic solvents such as toluene and hexane. By encapsulating metal cations, in what amounts to an organic cage, it is possible to apply solvent extraction to metal recovery.

The use of complexation to enhance solvent extraction is just one possible application for these ligands. Another useful application of ligand complexation is the separation of one metal from a mixture of metals.[6] Separation can be attained by complexation via ligands which

interact selectively with one metal from a mixture in solution. These ligands transform one metal more readily, so that extraction of this cation is facilitated. The relative distribution of the ions is then altered such that the organic phase contains a higher concentration of the targeted metal. Several passes through such a system would provide greater separation and therefore improve recovery. There are a wide variety of ligands which may be applied to separation and some have shown the capacity to recover a specific metal from fairly complex matrices.

By utilizing the distribution coefficients of the metals a separation coefficient, K, may be introduced. With K it is then possible to quantify the efficiency of separation:

$$K = \frac{D_M}{D_{M'}} \qquad [2]$$

where D_M and $D_{M'}$ are the distribution coefficients of the metals M and M'.

Currently, phosphine oxides are commercially

available for the selective recovery of some materials. For example, trioctylphosphine oxide extracts uranium from wet process phosphoric acid.[7] Although other examples of such systems exist, they are few in number and of limited use.[5] Since phosphine oxides lend themselves well to metal extraction a thorough investigation of this class of compounds could provide some very useful complexing ligands.

Exploring different phosphine oxide, metal and solvent combinations may be done through traditional laboratory experiments. However, it seems evident that a large number of such combinations are possible and, therefore, experimental determination would be inefficient. A less time consuming method would predict the affinity of a phosphine oxide for a particular metal and then predict the solubility of the metal complex in various solvents.[8] These data would then give an estimate of the distribution coefficient which could in turn be used to determine which ligands and solvents are worthy of further investigation.

B. Molecular mechanics

Molecular mechanics (MM)[9] may be used to estimate the distribution coefficient from the energy of the metal complex and the energy of the solvated complex. Comparison of the relative energies of various solvent, metal, and, ligand combinations would allow the elimination of high energy systems. Laboratory experiments would then be conducted only on those systems which are energetically promising.

i. Force field description

Molecular mechanics is an empirical computational method which treats molecules as a mechanical assembly of balls and springs. The system is based on Born's separation of nuclear and electronic motion, and formally treats only the nuclei. Hendrickson[10] proposed that the total energy of the molecule could be separated into a strain free component and a steric component. It is the steric energy component

upon which molecular mechanics is based.

$$E_{total} = E_{strain\ free} + E_{steric} \qquad [3]$$

The steric energy is broken up into terms which evaluate the increase in energy as atoms are moved from their optimal positions. These components evaluate steric energy, E_{steric}, as a function of deviation from optimal bond lengths ($E_{stretch}$), bond angles (E_{bend}), torsion angles ($E_{torsion}$), and Van der Waals separation (E_{VDW}). In some cases electrostatic (E_{elec}), and hydrogen bonding (E_{Hbond}), terms are included as well as some stretch and angle cross terms.

$$E_{steric} = E_{stretch} + E_{bend} + E_{torsion} + E_{VDW} + E_{elec} + E_{Hbond} \qquad [4]$$

The separate terms of the equation have been generated as a result of the amalgamation of vibrational spectroscopy, quantum mechanics and classical mechanics, such that the sum of the components is able to predict the change in energy associated with a change in internal coordinates.

The stretch term, $E_{stretch}$, is intended to reflect the increase in energy which occurs if a bond is stretched or

compressed from equilibrium. Figure ***i*** is an example of a typical energy curve for a pair of atoms which are moved from their ideal bond length.

A function which is commonly used to approximate the experimental behavior is the harmonic function:

$$E_{stretch} = \frac{1}{2} k(r-r_o)^2 \qquad [5]$$

where k is the stretching force constant, r is the bond length and r_o is the strain free bond length.

The harmonic function is based on Hooke's law and treats bonded atoms as particles bound together by an elastic spring. With this function there is no differentiation between compression of a bond and stretching of a bond. This assumption is true only for very small deviations from equilibrium and when the bond length lies far from equilibrium, the harmonic potential fails.

A more realistic representation of Figure ***i*** is the Morse function.[9]

$$E = D\{\exp[-(k/2D)^{1/2}(r-r_o)] - 1\}^2 \qquad [6]$$

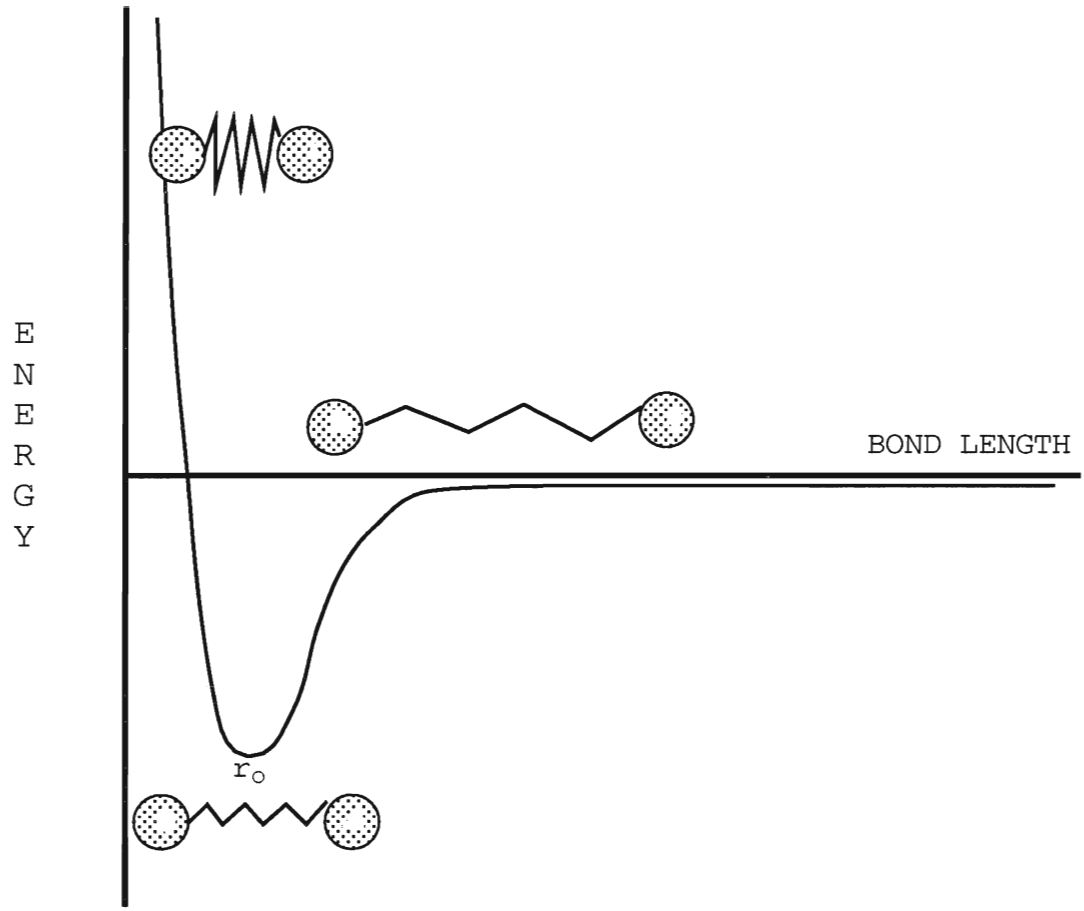

Figure i: ***Energy of a molecule as a function of bond length.***

where k is the stretching force constant, r is the bond length, r_o is the strain free bond length, and D is the bond energy. This representation takes anharmonicity into account but requires extended computation time.

Figure ***ii*** illustrates the behavior of the harmonic and Morse functions as the bond length changes. At a distance of less than 0.01Å from the strain-free value the two curves are neary indistinguishable. However, as the bond length increases, the cubic curve is considerably steeper than the Morse curve. Conversely as the bond length is compressed the Morse curve has a greater slope. Comparison of the two curves reveals that although both functions are suitable near the strain-free value the anharmonic behavior of the Morse function is more accurate away from equilibrium.

A compromise between efficiency and accuracy seems to be Allinger's cubic equation. This function contains an anharmonic component while at the same time being computationally efficient.[9]

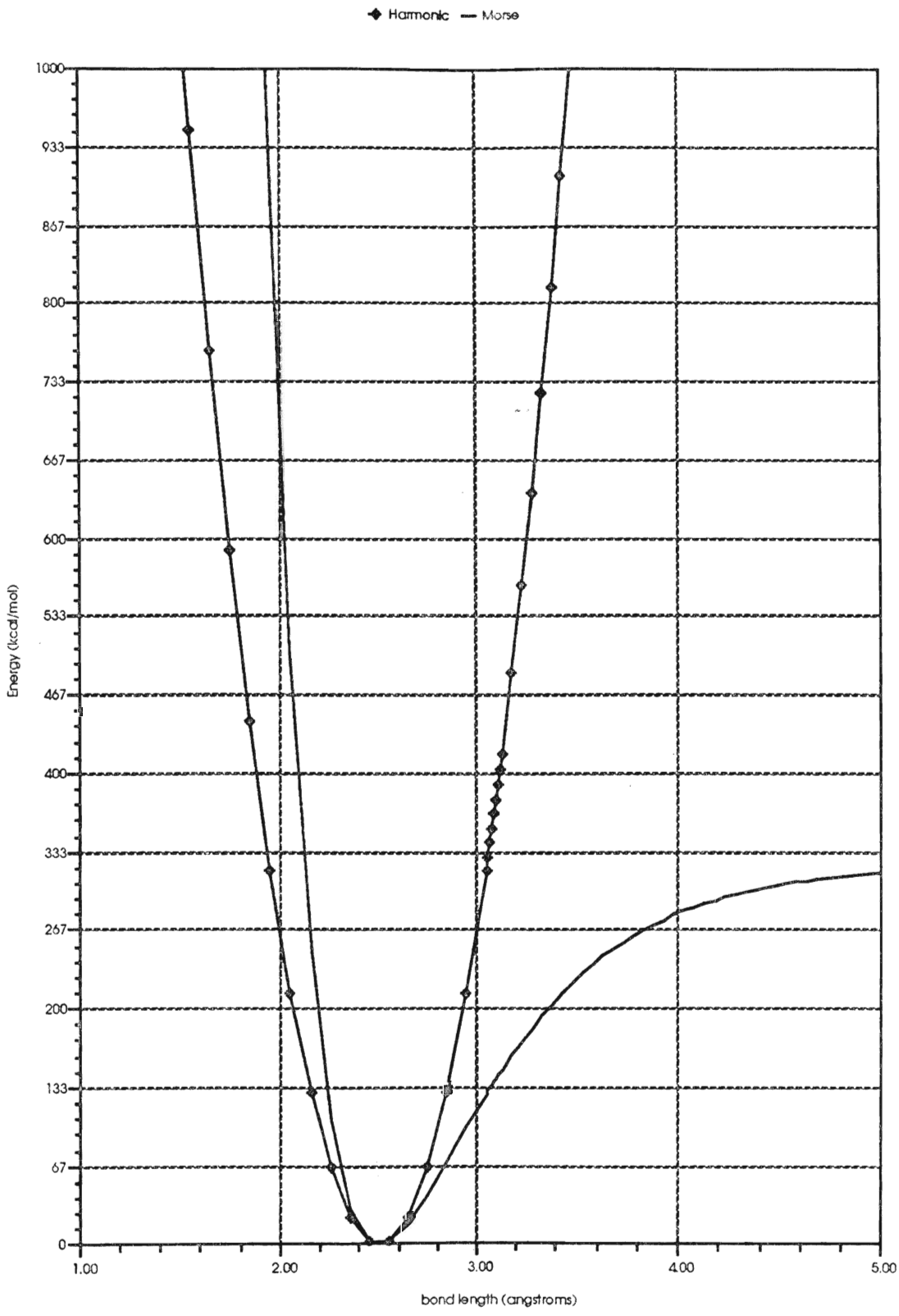

Figure ii: ***Comparison of the harmonic and Morse functions.*** When r is far from r_o the behaviour of the Harmonic energy term is incorrect.

$$E_{stretch} = \frac{1}{2} k[(r-r_o)^2+d(r-r_o)^3] \qquad [7]$$

where k is the stretching force constant, r is the bond length, r_o is the strain free bond length, and d is the cubic stretch constant.

While this function is convenient, care must be taken that the bond length is not too large as compared to the equilibrium bond length, (ie $r \not\approx r_o$). If this occurs the energy term continually improves as r approaches infinity and the molecule "dissociates". Some modeling programs modify Allinger's function to overcome this drawback. CHEM3DPlus[11] adds a fourth power term whereas BIOGRAF[12] changes the sign of the cubic term such that the energy continually increases with movement from equilibrium.

The bond angle term, E_{bend}, evaluates the increase in energy associated with movement away from a strain free bond angle. Here, again, Hookes law is often implemented.

$$E_{bend} = \frac{1}{2} k(\theta - \theta_o)^2 \qquad [8]$$

where k is the bending force constant, θ is the bond angle, and θ_o

is the strain free bond angle.

The harmonic approximation is not always a useful bond angle term and an alternative was introduced by Allinger. Allinger's function makes use of a sixth power term to increase the energy more sharply when the bond angle is far from the strain free value.[9]

$$E_{bend} = \frac{1}{2} k[(\theta - \theta_o)^2 + d(\theta - \theta_o)^6] \qquad [9]$$

where k is the bending force constant, θ is the bond angle, θ_o is the strain free bond angle, and d is the sixth power force constant.

It is also worthwhile to mention the cosine harmonic bond angle term. It has been found that a change in energy as a consequence of a change in bond angle, in some systems, is better approximated by this function.[13]

$$E_{bend} = \frac{1}{2} C(\cos\theta - \cos\theta_o)^2 \qquad [10]$$

where $C = (\sin^2\theta_o)/k$, k is the bending force constant and C is a modified force constant, θ is the bond angle, and θ_o is the strain free bond angle.

Functions which are equivalent to the cosine harmonic function are available in a truncated Fourier series.[13] These generalize the periodicity and allow for square planar and octahedral geometry by considering angles of 90° and 180° to be equivalent.

Some packages ignore all trans angles in order to simplify parameterization of certain coordination compounds. BIOGRAF has a default value, $E_{bend} = 0$, if $\theta > 135°$ which, in effect, eliminates all 180° angles. This approach has been found to cope well with angles about high coordination number (>4) metals.[14]

The barriers which hinder rotation about a bond are contained within a torsion angle term in molecular mechanics. For example Figure ***iii*** indicates that for butane, there exist several possible conformations, some of which are more favorable than others. The lowest energy occurs when the methyl groups are anti to one another, that is, they are at a torsion angle of 180°. The quantity of energy required for conversion from the

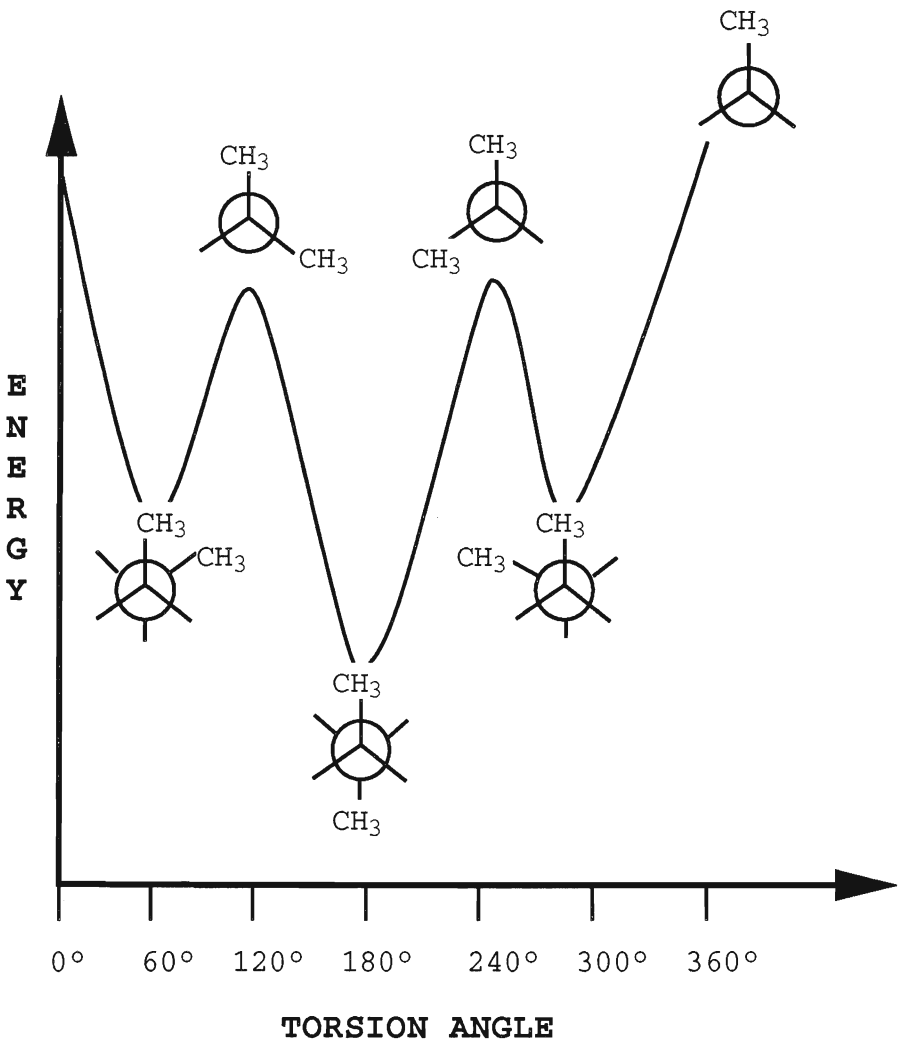

Figure iii: ***Energy of a butane molecule as a function of the torsion angle.***

anti isomer to a less favored gauche isomer is represented by a torsion barrier. The function that best reproduces the energy surface of the transition between different conformations is a Fourier series:

$$E_{\phi} = \sum_{n=1}^{p} \tfrac{1}{2} k_{\theta,n}(1-d\cos n\phi) \qquad [11]$$

where n=1,2,...,6 and defines the period, d=±1 and is used to define the location of the maximum or minimum, $k_{\theta,n}$ is the rotational energy barrier, and ϕ is the torsion angle.

The van der Waals term, E_{VDW}, is required to emulate the relationship between two bodies which are attracted to one another at long range and repelled by one another at short range (Figure ***iv***). The function must, therefore contain an attractive component as well as a repulsive component each of which dominates at the appropriate distances.

$$E_{vdw} = E_{repulsive} + E_{attractive} \qquad [12]$$

The attractive component has been demonstrated to have an r^{-6} dependence[14-16] and most force fields incorporate this

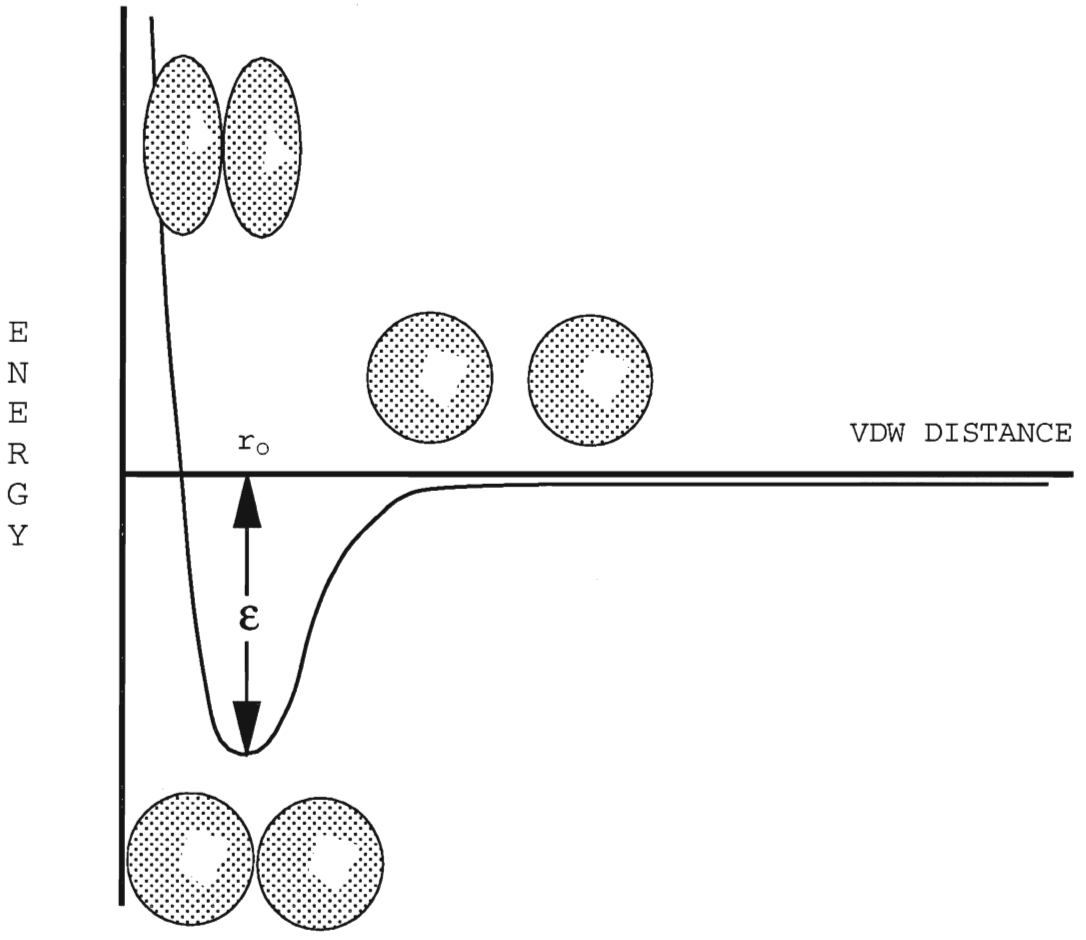

Figure iv: ***Energy of a molecule as a function of the van der Waals radii***

relationship into the van der Waals function. The repulsive component is not as well established and several functions are considered suitable.

The Lennard-Jones potential is often found in molecular mechanics, usually with a repulsive exponent of 12 and an attractive exponent of 6.[9]

$$E_{vdw} = \varepsilon[(r_o/r)^{12} - 2\ (r_o/r)^{6}] \qquad [13]$$

where ε defines the depth of the potential well, r is the distance between the atoms and r_o is the minimum energy distance.

An alternative which was found to better reproduce the short range interactions is a modified Buckingham potential function.[16]

$$E_{vdw} = \varepsilon[\frac{6}{\zeta-6} e^{\zeta(1-r/r_o)} - \frac{6}{\zeta-6}(r_o/r)^{6}] \qquad [14]$$

where ε defines the depth of the potential well, ζ is a dimensionless scaling constant, r is the distance between the atoms and r_o is the minimum energy distance.

The van der Waals term is calculated for atoms which have a 1,4 separation or greater and are considered to be non-bonded interactions. The 1,2 and 1,3 contacts are not included in van der Waals calculations since it is assumed that $E_{stretch}$ incorporates the 1,2 interactions and E_{bend} the 1,3 interaction. Although 1,4 interactions are included in the torsion angle term as well, it was found that without both 1,4-terms, the molecular mechanics force fields could not be made to accurately reproduce the relative energies of different conformers in a given molecule.[9]

ii. Minimization

With the wide variety of force fields available it is possible to predict the steric energy for a large number of compounds. However, in order for molecular mechanics to be useful, the technique must provide the lowest energy geometries, as well as calculate the energy of those geometries. Finding the lowest energy isomer or conformer requires finding the

global minimum of the potential energy surface.

One method to locate an energy minimum involves using the first derivative[9]. A second method involves both the first derivative of the potential energy surface, as well as the second derivative.[9] It is important to note, however, that regardless of how efficient these methods are at finding the minima, local minima only are found. There is no direct method for finding the global minimum and care must be taken that structures which lie at local minima are not mistaken for the lowest energy configuration. The minimum located is usually the one closest to the starting point, rather than the global minimum.

The first derivative method is known as the method of steepest descents (Figure ***v***). This method systematically changes the starting coordinates, (x_0,y_0,z_0), of each atom by a pre-set distance (normally 0.001Å) to a new set of coordinates, (x_1,y_1,z_1). The energy of the second coordinate set is compared to the original. All coordinate changes which increase the

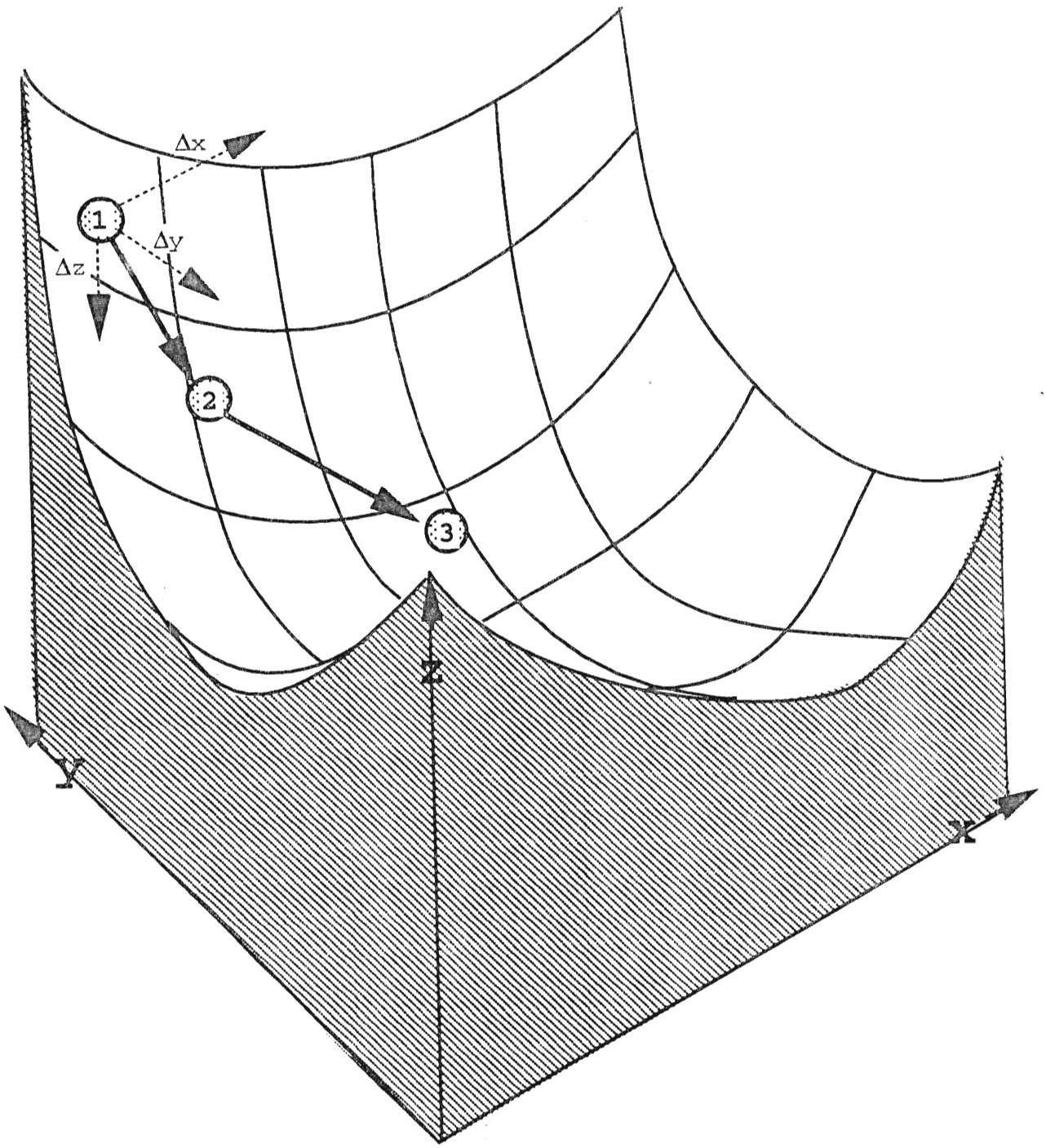

Figure v: ***Method of steepest descents for locating potential energy minima.***

The slope of all combinations of Δx, Δy and Δz at 1 is evaluated and the steepest value is selected as the path to 2. This process is repeated until the minimum is reached.

steric energy of the molecule are discarded. The coordinates which decrease the total energy are then used as the starting point for the next set of trials. In order to reach the minimum at a faster rate, the slopes of the potential energy at the initial and trial coordinates are compared. The slope with the steepest gradient is chosen as the path to the minimum. The process is repeated until the slope reaches some pre-set limit such as 0.1 kcal/molÅ.

The second derivative method is known as the Newton-Raphson method and utilizes the function:

$$x_1 = x_0 - \frac{f'(x_0)}{f''(x_0)} \qquad [15]$$

To find x_1 the slope of the potential energy surface is evaluated to give $f'(x_0)$. Figure ***vi*** depicts the process. The tangent of $f'(x_0)$ intersects the x-axis at x_1. This value of x_1 is then substituted for x_0 in equation 15 and the differentiation process is repeated. When the tangent to the first derivative intersects both the x axis and the first

1. form of the potential energy surface

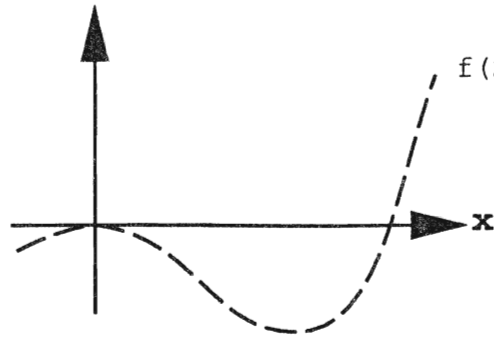

2. derivative of the surface

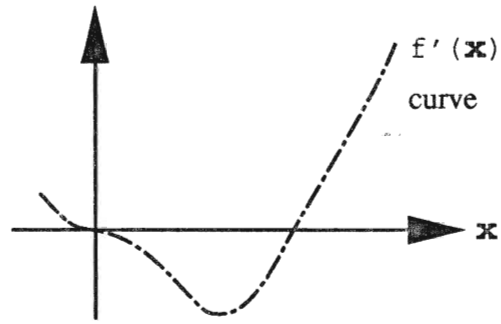

3. finding x_1 using the tangent @ x_o

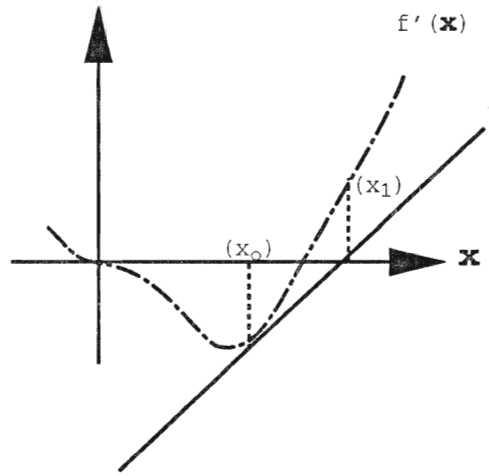

4. using x_1 to find x_2 . . .

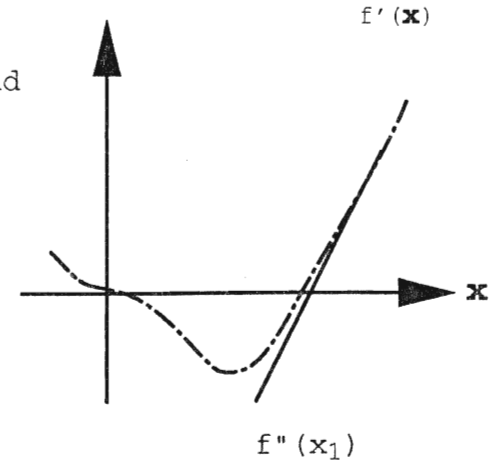

Figure vi: ***Newton-Raphson method for locating potential energy minima.***

derivative at the same point the local extreme has been located.

Each of the two methods has advantages and drawbacks. The method of steepest descents works quickly at steep gradients, far from the minimum, but is slow near the minimum. Conversely, the Newton-Raphson method works well near the minimum but less so, far from the minimum. It is possible to use a combination of the two methods outlined, or select one or the other, depending on the confidence of the starting structure and hardware restrictions.

C. Metal complexes of phosphine oxide

The ultimate goal of modeling metal-phosphine oxide complexes is to establish a set of parameters which could perform with any given phosphine oxide complex. However, building such a force-field is a stepwise process and a starting point must be selected. A practical starting point would be to accumulate a set of compounds which are large

enough in number to test accuracy and transferability while at the same time being manageable. The group of compounds chosen to represent metal phosphine oxides was a set of tin bis-triphenylphosphine oxide complexes, each containing a variable number of ethyl and halogen groups.

Initially four chlorine containing structures were obtained: trans-$SnCl_2Et_2(tppo)_2$[17], cis-$SnCl_2Et_2(tppo)_2$[17], trans-$SnCl_3Et(tppo)_2$[18], and cis-$SnCl_4(tppo)_2$[19]. The two $SnCl_2Et_2(tppo)_2$ molecules were dismissed after closer inspection due to a significant number of errors in the crystal coordinates provided. Figures ***vii*** and ***viii*** provide the structure of the chloro-tin-phosphine oxide complexes as well as their nomenclature.

Similarly, three bromine containing structures were obtained. Trans-$SnBr_2Et_2(tppo)_2$[20] was later omitted from some experiments due to difficulties which were encountered in creating the extended crystal structures. The two molecules, trans-$SnBr_3Et(tppo)_2$[21] and trans-$SnBr_4(tppo)_2$[22], were, however,

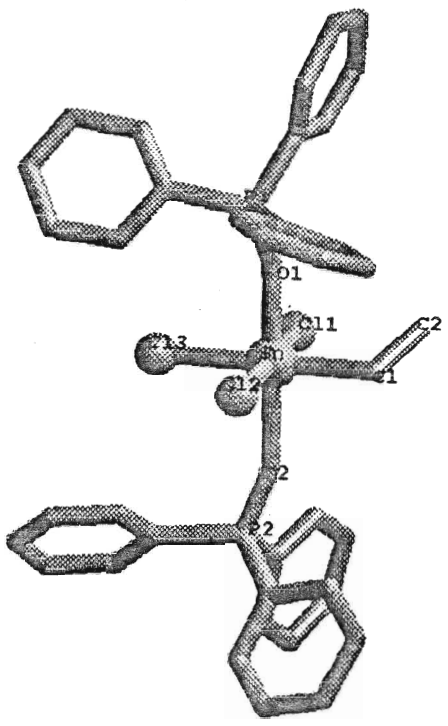

Figure vii: $SnCl_3Et(tppo)_2$.

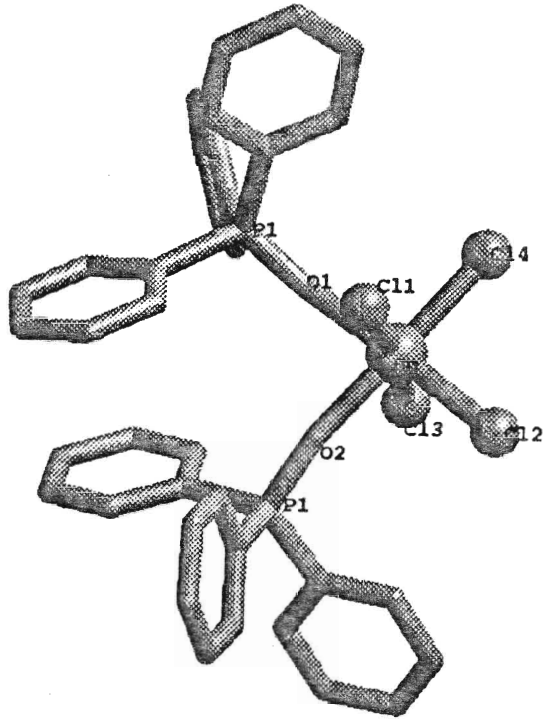

Figure viii: $SnCl_4(tppo)_2$.

maintained throughout the experiments. All three molecules are illustrated in Figures ***ix - xi.***

The three iodide derivatives obtained were all usable and were therefore included in the experiments. The compounds were: trans-$SnI_2Et_2(tppo)_2$[23], trans-$SnI_3Et(tppo)_2$[24] and cis-$SnI_4(tppo)_2$[25] and they can be seen in Figures ***xii- xiv.***

Table ***I*** shows some of the parameters of these compounds which are expected to introduce difficulties in the

Molecule	R	Sn-X	Sn-O-P	Reference
trans-$Cl_3Et(tppo)_2$	0.063	2.487Å 2.498Å 2.360Å	148.3° 158.3°	18
cis-$Cl_4Et(tppo)_2$	0.027	2.386Å 2.390Å 2.379Å 2.387Å	157.2° 157.2°	19
trans-$SnBr_3Et(tppo)_2$	0.091	2.654Å 2.652Å 2.504Å	155.2° 158.3°	21
trans-$SnBr_4(tppo)_2$	0.049	2.511Å 2.584Å 2.576Å 2.558Å	160.1° 151.7°	22
trans-$SnI_2Et_2(tppo)_2$	0.053	2.916Å 3.127Å	150.1° 167.2°	23
trans-$SnI_3Et(tppo)_2$	0.051	2.895Å 2.957Å 2.723Å	155.6° 159.2°	24
cis-$SnI_4(tppo)_2$	0.050	2.835Å 2.712Å 2.654Å 2.951Å	152.0° 161.4°	25

Table I: ***Bond lengths and angles.***

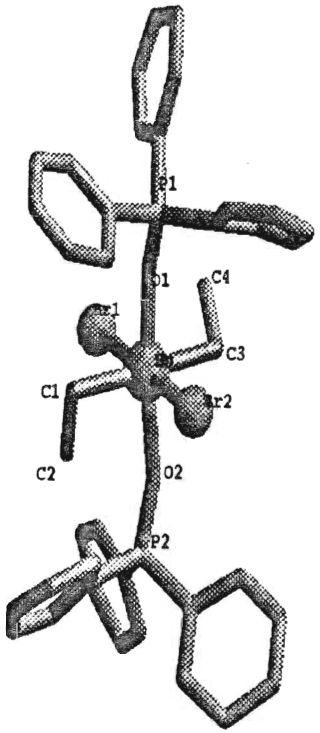

Figure ix: $SnBr_2Et_2(tppo)_2$

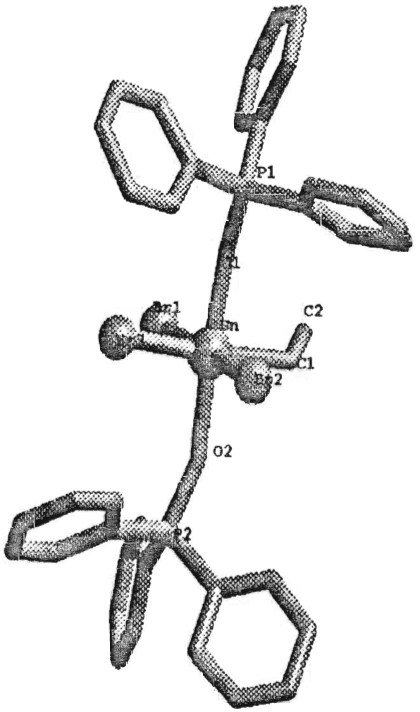

Figure x: $SnBr_3Et(tppo)_2$

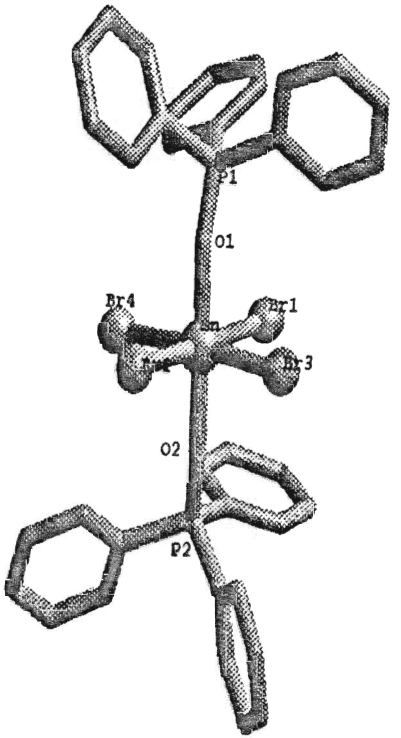

Figure xi: $SnBr_4(tppo)_2$

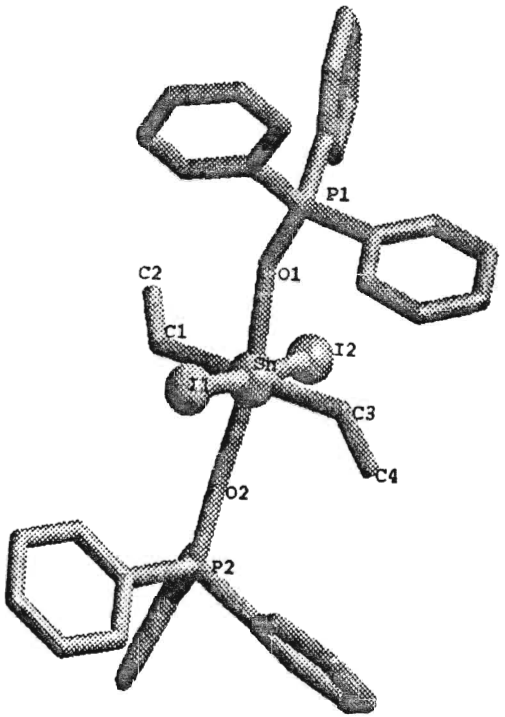

Figure xii: ***$SnI_2Et_2(tppo)_2$***

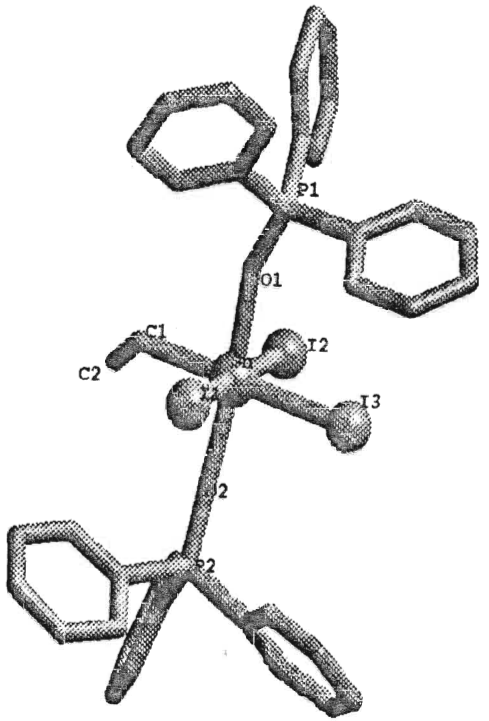

Figure xiii: ***$SnI_3Et(tppo)_2$***

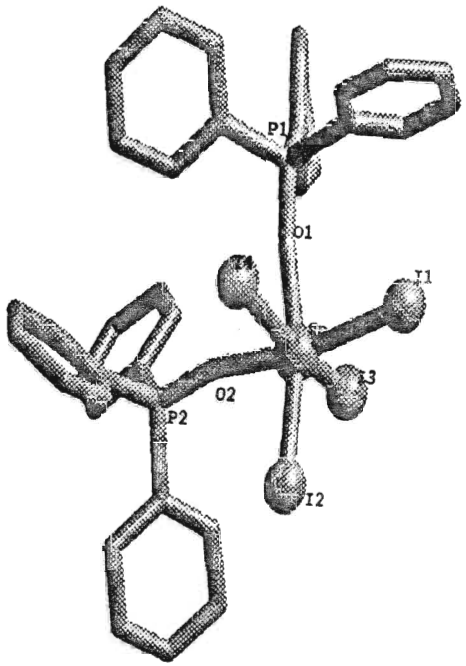

Figure xiv: ***$SnI_4(tppo)_2$***

parameterization. The R-factor is also included to provide an indication of the precision of the crystal coordinates. It is anticipated that the wide distribution of these bond lengths and angles will prove problematic. For example, the Sn-Cl bond lengths vary from 2.360 Å to 2.498 Å. For this 0.138 Å spread only one strain-free value can be substituted into the stretch term. Similarly the Sn-O-P angles are expected to present even greater difficulties since these values vary by as much as 19° and, again, only one strain free value is contained in the bond angle term.

In order to apply molecular mechanics, generally an organic chemist's tool, to these coordination complexes the range of options available with the software package must be explored. Various force constants, analytic potential functions and crystal packing arrangements are available which can be combined to expand the scope of molecular mechanics to include inorganic compounds.[26] By incorporating these options, treatment of metal-phosphine oxide complexes

can provide results comparable to those achieved in the analysis of the traditional organic molecules.

II. EXPERIMENTAL

A. Compounds

Initially a suitable group of compounds on which to conduct preliminary calculations was selected. This was done through the Cambridge Crystallographic Database[27], which provided a list of all structures containing a metal-oxygen-phosphorus group. From this list a class of compounds which contained: tin, triphenylphosphine-oxide, and various halogens was selected based on the total number of compounds available, and the presence of the desired functional groups.

Molecular mechanics calculations were conducted with the BIOGFRAF computational package from Molecular Simulations Incorporated.[12] Allinger's MM2 forcefield[28,29] was used as the default for energy calculations.

The Cambridge Crystallographic Database[27] supplied not only the names and bibliographic information of the necessary compounds, but also their crystal coordinates and

accompanying symmetry information. This data was downloaded directly into text files and edited to provide files compatible with the software format.

B. Parameterization

Parameterization was essentially a four step process the complexity of which increased as was required to improve the fit. The four steps were:

i. use of all parameters available with BIOGRAF and estimation of missing parameters

ii. optimize the new parameters

iii. survey possible analytic functions

iv. explore the effects of crystal packing

i. BIOGRAF parameters and estimation of missing parameters

Parameters provided with the force field were retained without change. All functions for stretch, bend, torsional and non-bonded interactions initially used were the

default provided with the MM2 force field.

Missing strain free bond lengths for Sn-O and Sn-X were initially selected as the minimum value of all equivalent observed bond lengths when harmonic functions were utilized. With anharmonic functions the median value of the set was used. A similar process was repeated for the missing bond angles. Missing stretch and bend force constants were tentatively selected by assuming transferability from similar compounds. Missing tin halogen and tin oxygen stretch constants were transferred from the corresponding carbon bond lengths. Missing XSnX bending force constants were set at values similar to constants for existing 90° bond angles. The SnOP bending force constant was set at an arbitrarily low value. In some cases the choice of force constants was substantiated using vibrational spectra of hexahalostannates.

The torsional parameters which involved tin were set to approximately zero as is common practice for octahedrally coordinated metals.[30] BIOGRAF does not allow a value of zero

for the torsion term, so in most cases the closest possible number was selected, 0.001. In some instances a value of 0.1 was used in combination with a six-fold barrier. This was done to provide the correct number of minima while at the same time maintaining a low energy barrier for motion between configurations.

ii. Optimization

The starting set of parameters were tested by conducting an energy minimization. The geometry of the observed structure and the minimized structure were compared. Any bond lengths, angles and torsions which were not satisfactorily matched had their parameters adjusted to improve the fit. This process was repeated until no further improvement was observed.

iii. The analytic functions

When it was found that the normal MM2 force field

functions failed to duplicate the geometry, alternative functions available with the software were considered. A cosine harmonic function was found more suitable for the SnOP bond angle term and a Morse function was used for the tin to halogen stretch terms. Tables ***II,III*** and ***IV*** list all of the parameters used for the final calculations. Those parameters not included in Allinger's set are highlighted.

iv. Crystal packing

The effect of a "solid" environment, rather than the traditional "gas" system, was explored. That is, the isolated molecule was packed with its nearest neighbors, as would be observed in the crystal structure.

Surrounding the central molecules initially involved obtaining the nearest neighbors. The X-ray coordinates as received from the Cambridge Crystallographic Database were used to plot the core molecule. The space group was then used to find the symmetry operations which would generate all other

BONDS	TYPE	K_r	r_o	D or d
C_3 -H__C	cubic	661.848	1.1130	-2.0
C_3 -C_3	cubic	633.072	1.5230	-2.0
C_2R -H__C	cubic	661.848	1.1010	-2.0
C_2R -C_3	cubic	633.072	1.4970	-2.0
C_2R -C_2R	cubic	450.0	1.3	-2.0
P_3 -O_2+	cubic	200.0	1.495	-2.0
P_3 -C_2R	cubic	460.0	1.775	-2.0
Sn -C_3	**cubic**	**306**	**2.149**	**-2.0**
Sn -Cl	**Morse**	**10**	**2.55**	**77.0**
Sn -Br	**Morse**	**15**	**2.67**	**65.0**
Sn -I_	**Morse**	**15**	**2.90**	**50.0**
Sn -O_2+	**cubic**	**145**	**2.16**	**-2.0**

Table II: ***Analytic functions and parameters used for bond stretching:***
K_r is in kcal/molÅ^2, r_o is in Å, D is in kcal/mol and d is in kcal/molÅ

Bold type signifies parameters not included with MM2 forcefield

ANGLE	TYPE	K_θ	θ_o
H__C -C_3 -H__C	sextic	46.0	109.4
C_3 -C_3 -H__C	sextic	51.8	109.4
Cl -Sn -H__C	**sextic**	**72.0**	**90.0**
Cl -Sn -D__C	**sextic**	**72.0**	**90.0**
Cl -Sn -F_	**sextic**	**72.0**	**90.0**
I_ -Sn -I_	**sextic**	**57.6**	**90.0**
Br -Sn -Br	**sextic**	**57.6**	**90.0**
C_3 -Sn -C_3	**sextic**	**19.0**	**90.0**
O_2+ -Sn -O_2+	**sextic**	**72.0**	**90.0**
O_2+ -Sn -Cl	**sextic**	**72.0**	**90.0**
O_2+ -Sn -Br	**sextic**	**72.0**	**90.0**
O_2+ -Sn -I_	**sextic**	**72.0**	**90.0**
O_2+ -Sn -C_3	**sextic**	**72.0**	**90.0**
C_3 -Sn -Br	**sextic**	**72.0**	**90.0**
C_3 -Sn -Cl	**sextic**	**72.0**	**90.0**
C_3 -Sn -I_	**sextic**	**72.0**	**90.0**
Cl -Sn -Cl	**sextic**	**57.6**	**90.0**
Cl -Sn -Cl	**sextic**	**57.6**	**90.0**
H__C -C_3 -Sn	**sextic**	**72.0**	**109.0**
C_3 -C_3 -Sn	**sextic**	**37.0**	**109.0**
Sn -O_2+ -P_3	**cos harm**	**37.0**	**140.0**
O_2+ -P_3 -C_2R	sextic	65.0	109.0
C_2R -C_2R -C_2R	sextic	62.0	120.0
P_3 -C_2R -H__C	sextic	52.0	120.0
P_3 -C_2R -C_2R	sextic	52.0	120.0
C_2R -P_3 -C_2R	sextic	57.0	109.0
C_2R -C_2R -H__C	sextic	52.0	120.0

Table III: ***Analytic functions and parameters used for bond angle bending.***

K_θ is in kcal/molrad^2 and θ_o is in degrees.
The sixth power term is 0.754337 rad^{-4}

Bold type signifies parameters not included with MM2 forcefield

Torsion	$k_{\theta n}$	n	d
H__C -C_3 -C_3 -H__C	0.237	3	-1
H__C -C_2R -C_2R -H__C	10.000	2	1
C_2R -C_2R -C_2R -H__C	-1.060	3	1
	9.000	2	1
C_2R -C_2R -C_2R -C_2R	8.000	2	1
	-0.93	1	1
P_3 -C_2R -C_2R -H__C	16.250	2	1
P_3 -C_2R -C_2R -C_2R	16.250	2	1
C_2R -P_3 -C_2R -C_2R	0.3300	2	1
C_2R -P_3 -C_2R -H__C	0.3300	2	1
C_3 -C_3 -Sn -O_2+	**0.0100**	**4**	**1**
C_3 -C_3 -Sn -Br	**0.0100**	**4**	**1**
C_3 -C_3 -Sn -I_	**0.0100**	**4**	**1**
C_3 -C_3 -Sn -Cl	**0.0100**	**4**	**1**
C_3 -C_3 -Sn -C_3	**0.0100**	**4**	**1**
I_ -Sn -O_2+ -P_3	**0.1000**	**6**	**-1**
Cl -Sn -O_2+ -P_3	**0.1000**	**6**	**-1**
Br -Sn -O_2+ -P_3	**0.1000**	**6**	**-1**
O_2+ -Sn -O_2+ -P_3	**0.1000**	**6**	**-1**
C_3 -Sn -O_2+ -P_3	**0.1000**	**6**	**-1**
H__C -C_3 -C_3 -Sn	**0.0010**	**3**	**1**
Sn -O_2+ -P_3 -C_2R	**0.0010**	**3**	**1**
O_2+ -P_3 -C_2R -C_2R	**0.0010**	**3**	**1**
C_3 -C_3 -Sn -H__C	**0.0010**	**6**	**1**
H__C -C_3 -Sn -O_2+	**0.0010**	**6**	**1**
H__C -C_3 -Sn -C_3	**0.0010**	**6**	**1**
H__C -C_3 -Sn -Cl	**0.0010**	**6**	**1**
H__C -C_3 -Sn -Br	**0.0010**	**6**	**1**
H__C -C_3 -Sn -I_	**0.0010**	**6**	**1**
O_2+ -P_3 -C_2R -H__C	**0.0010**	**3**	**1**

Table IV: ***Analytic functions and parameters used for Torsion angles.*** $k_{\theta n}$ is in kcal/mol. Bold type signifies parameter not included with MM2

molecules in the unit cell. Finally the unit cell was replicated in ±x,±y and ±z direction. This produced a large number of surrounding molecules, (approximately 60), of which all but the 20 closest were eliminated. These were 7Å to 18Å from the core. After visual inspection, all molecules not part of the first shell were eliminated. This provided a central core with the desired sized shell about it containing between 12 and 16 neighbors. Figure ***xv*** depicts the various layers for $SnBr_4(tppo)_2$. The layer in the plane of the core molecule is shown, as well as the layers above and below the core. Figures ***xvi*** to ***xxii*** depict the configuration of the packing for all the structures analyzed. Energy and geometric information relating to the central molecule was retrieved by simply removing the outer shell and conducting an energy and geometric analysis of the isolated molecule.

The criteria chosen to evaluate the parameters was based on the correlation of geometry between the starting structures and the minimized structures. If the bond lengths, bond angles and torsion angles of the minimized structure fell

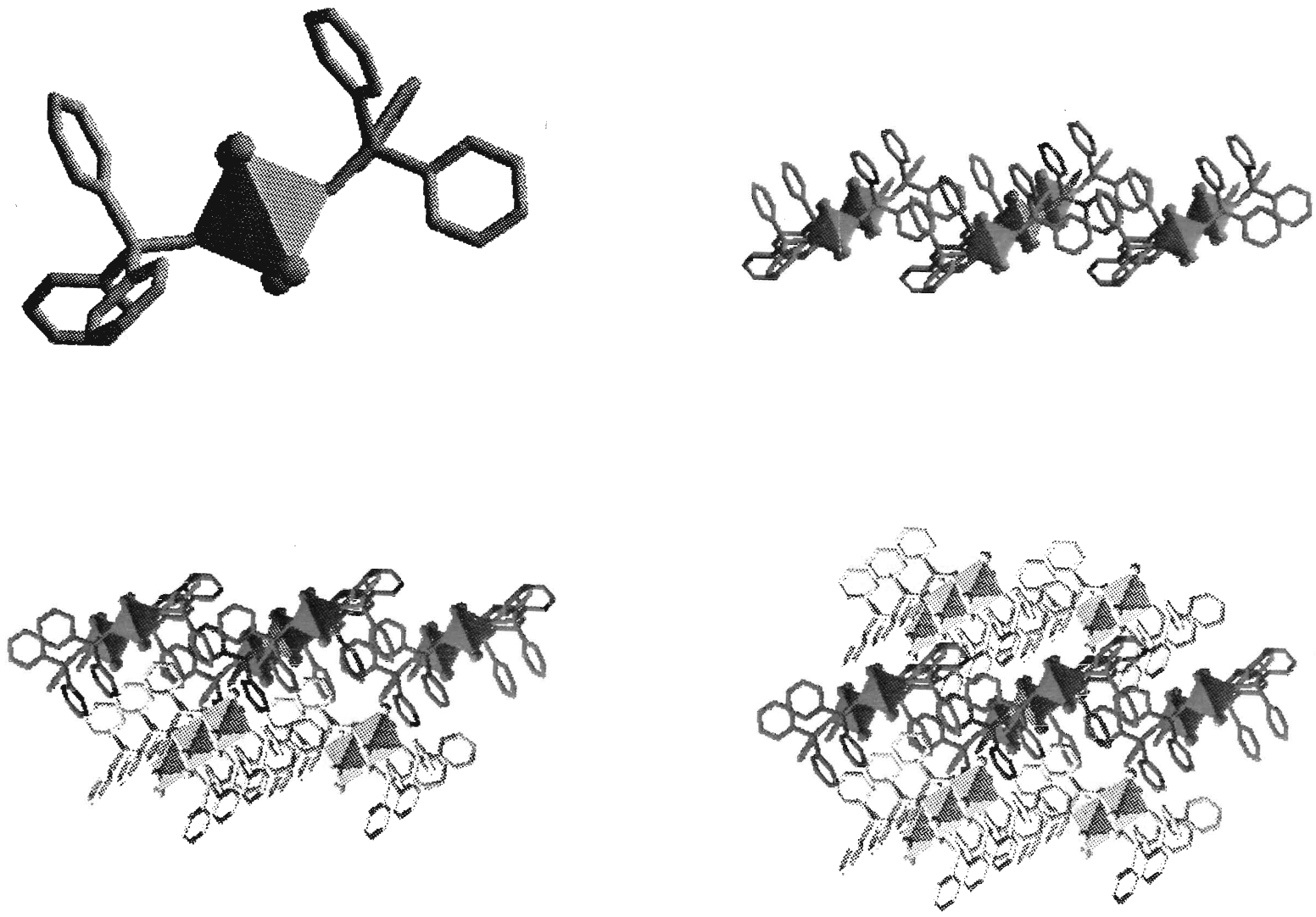

Figure xv: ***Layers about, below and above the isoleated molecule.***

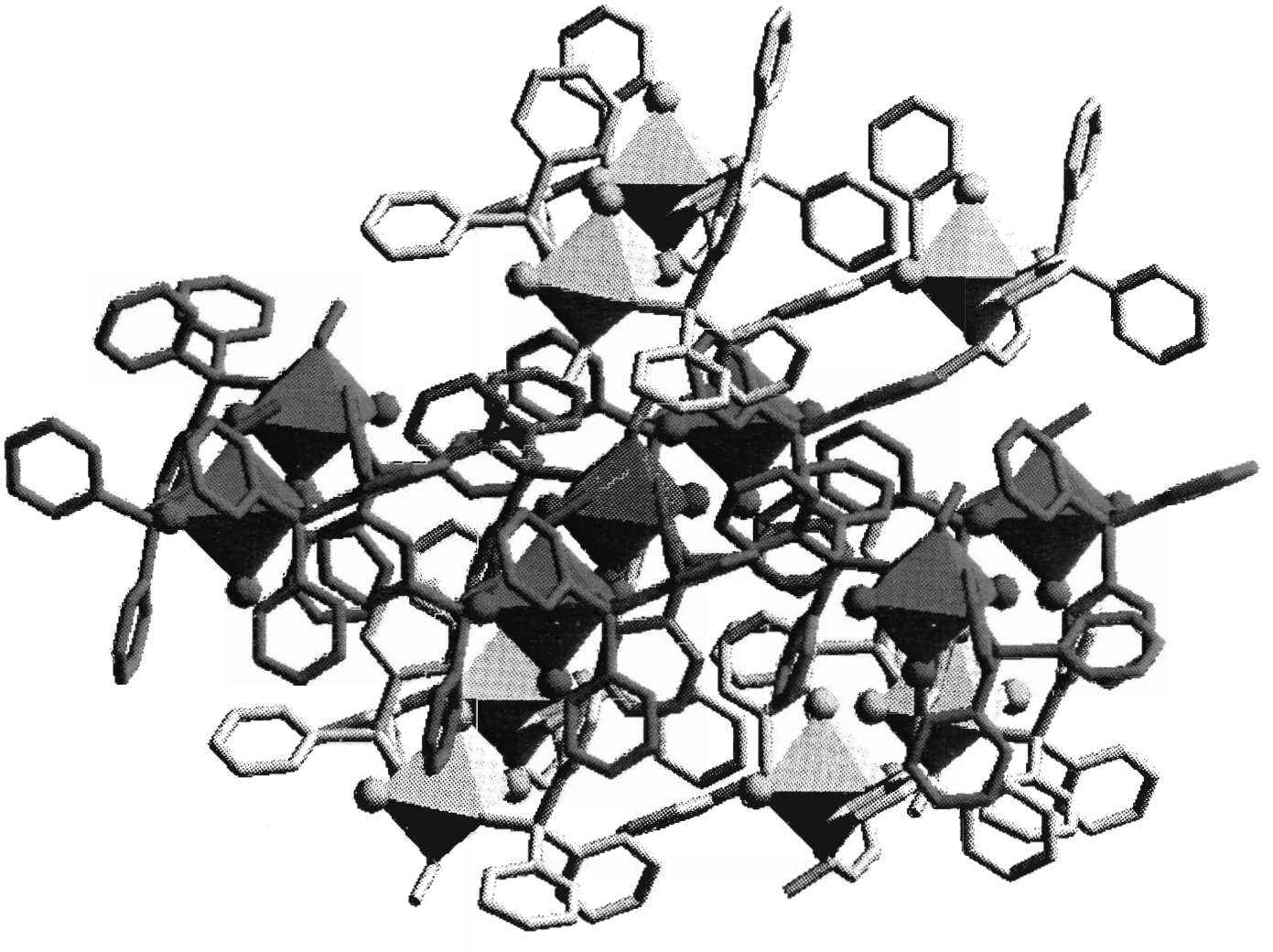

Figure xvi:***Crystal packed $SnCl_3Et(tppo)_2$***

Figure xvii: ***Crystal packed $SnCl_4(tppo)_2$***

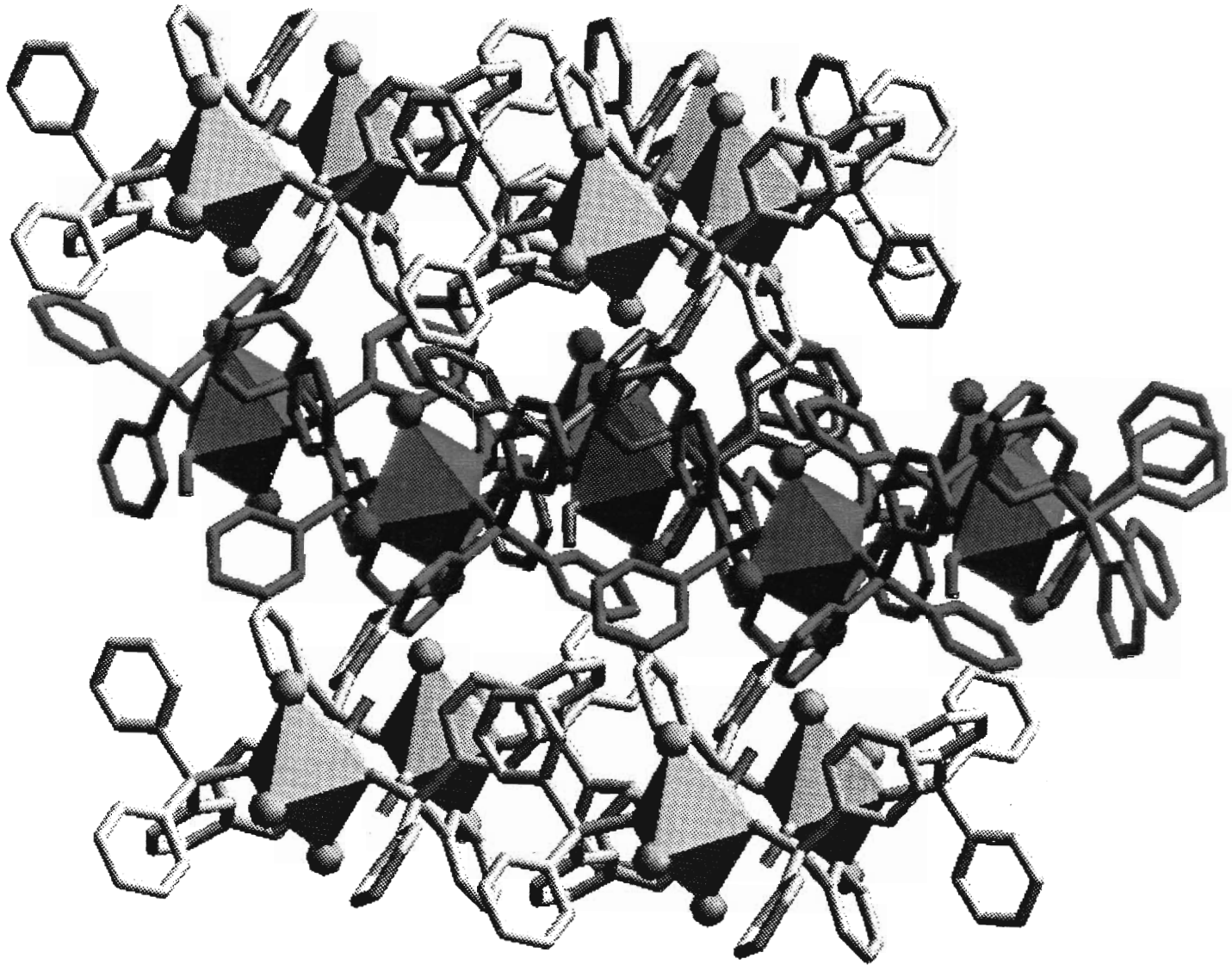

Figure xviii: ***Crystal packed $SnBr_3Et(tppo)_2$***

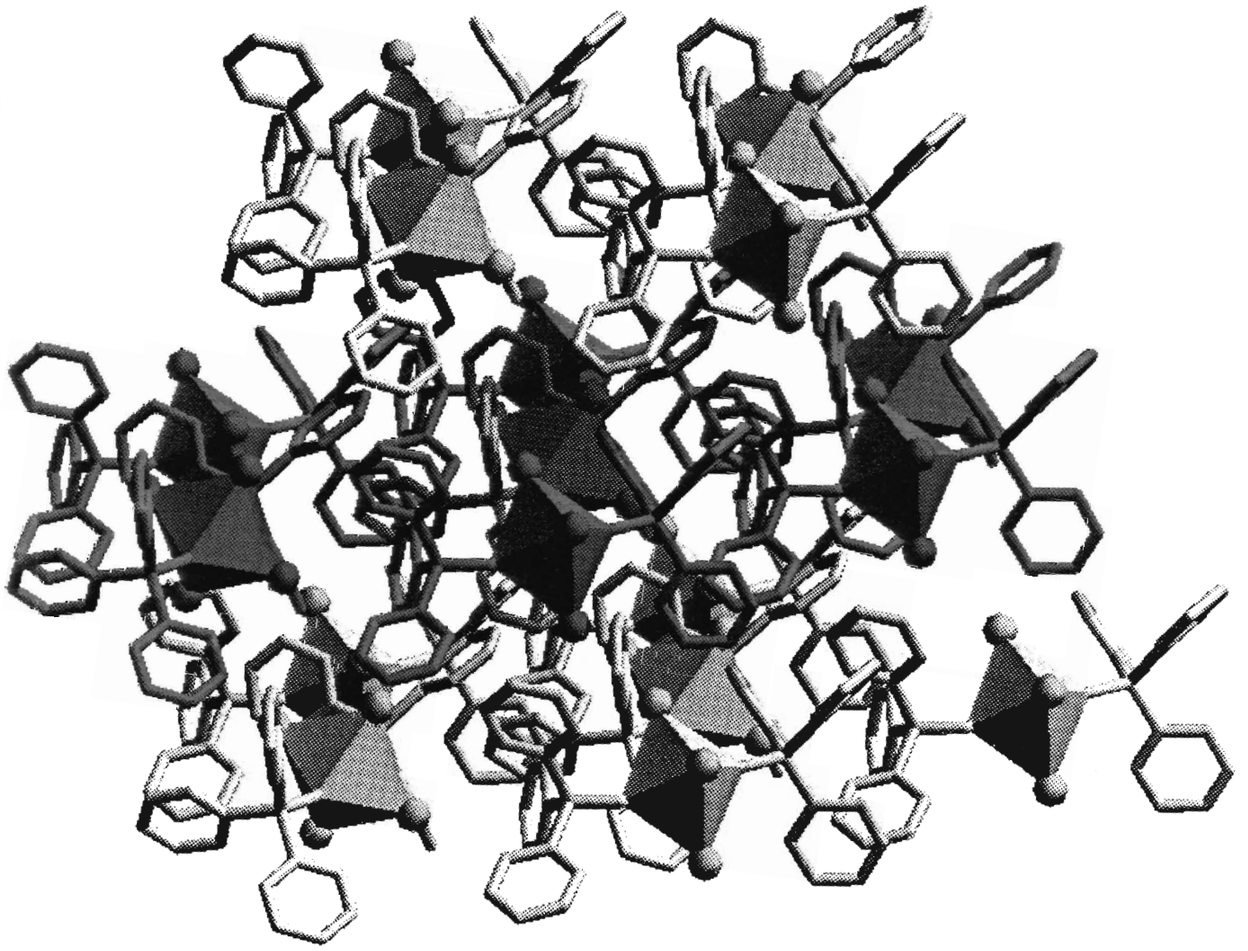

Figure xix: ***Crystal packed $SnBr_4(tppo)_2$***

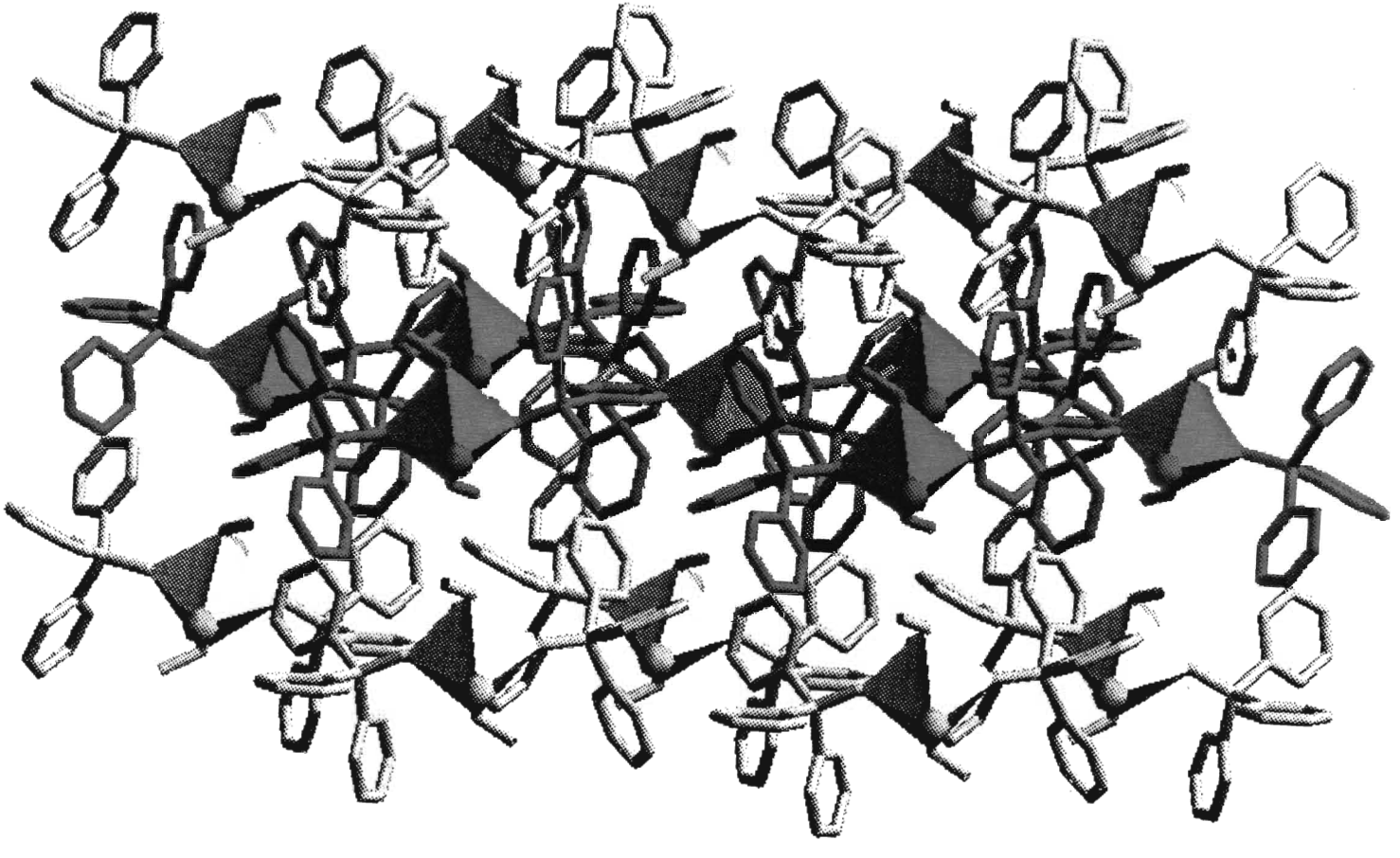

Figure xx: ***Crystal packed $SnI_2Et_2(tppo)_2$***

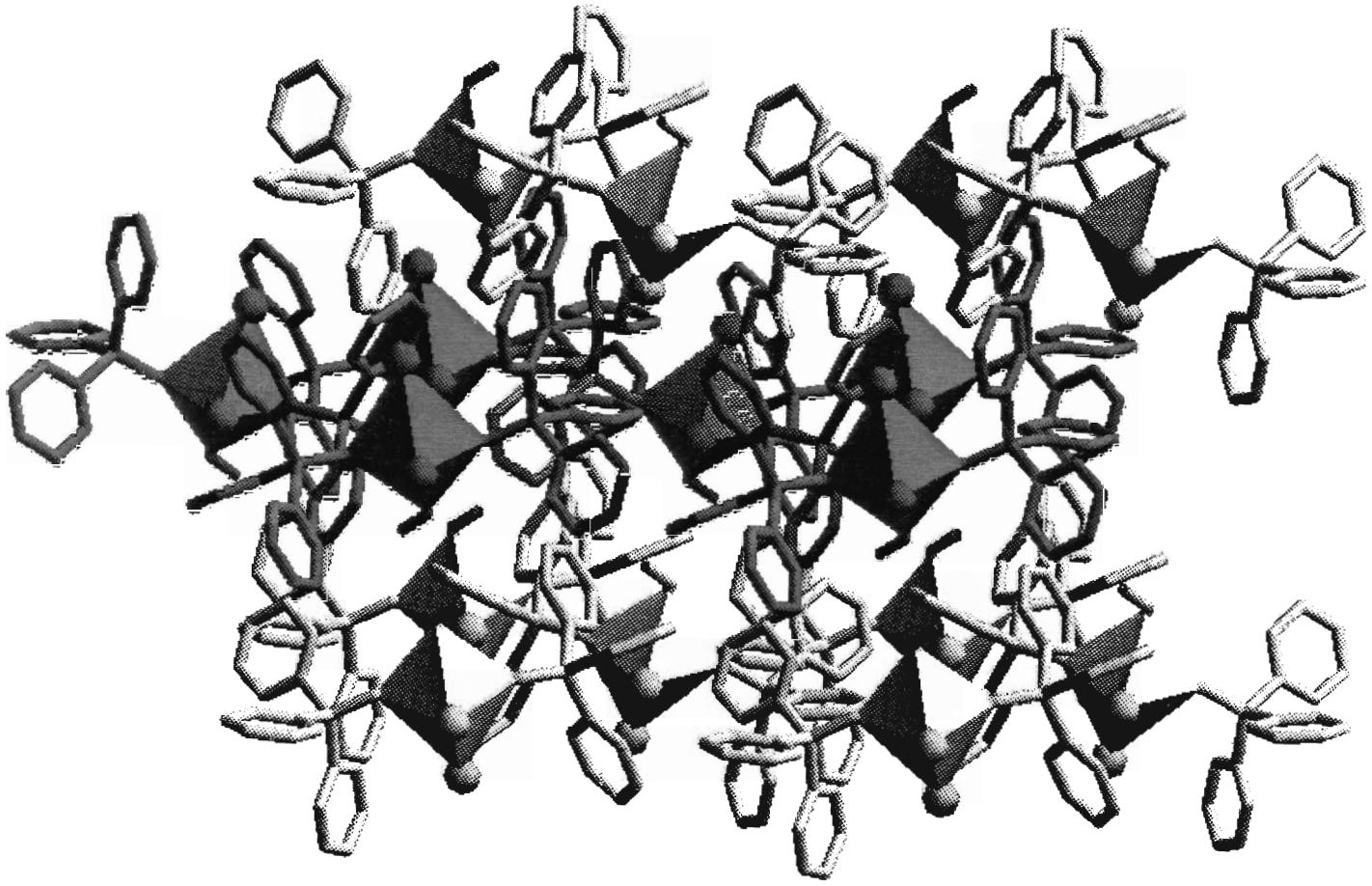

Figure xxi: ***Crystal packed $SnI_3Et(tppo)_2$***

Figure xxii:***Crystal packed $SnI_4tppo)_2$***

within a suitable margin of error, the parameters were considered satisfactory. It would have been preferable to also have energy information for comparison but this was not available to us.

III. RESULTS AND DISCUSSION

A. MM and the MOP bond angle

i. Description of the P-O bond

In the attempt to model phosphine oxides with molecular mechanics the metal-oxygen-phosphorus (MOP) bond angle has proved to be the most difficult parameter to reproduce. This difficulty is partially due to the fact that the nature of the oxygen-phosphorus bond has not yet been clearly defined. It has been proposed that M-O-P, M-O=P, and M-O≡P bonding is possible. If bonding were M-O-P an MOP bond angle of 109° would be expected. If bonding were M-O=P an MOP bond angle of 120° would be expected and if the O to P bond were considered a triple bond an angle of 180° would be expected.

Experimentally, the MOP angle varies from 130° to 180°. These data were obtained from a search of the Cambridge Crystallographic Database,[27] and are presented in Figure ***xxiii***. No conclusions about the bonding type can be made from

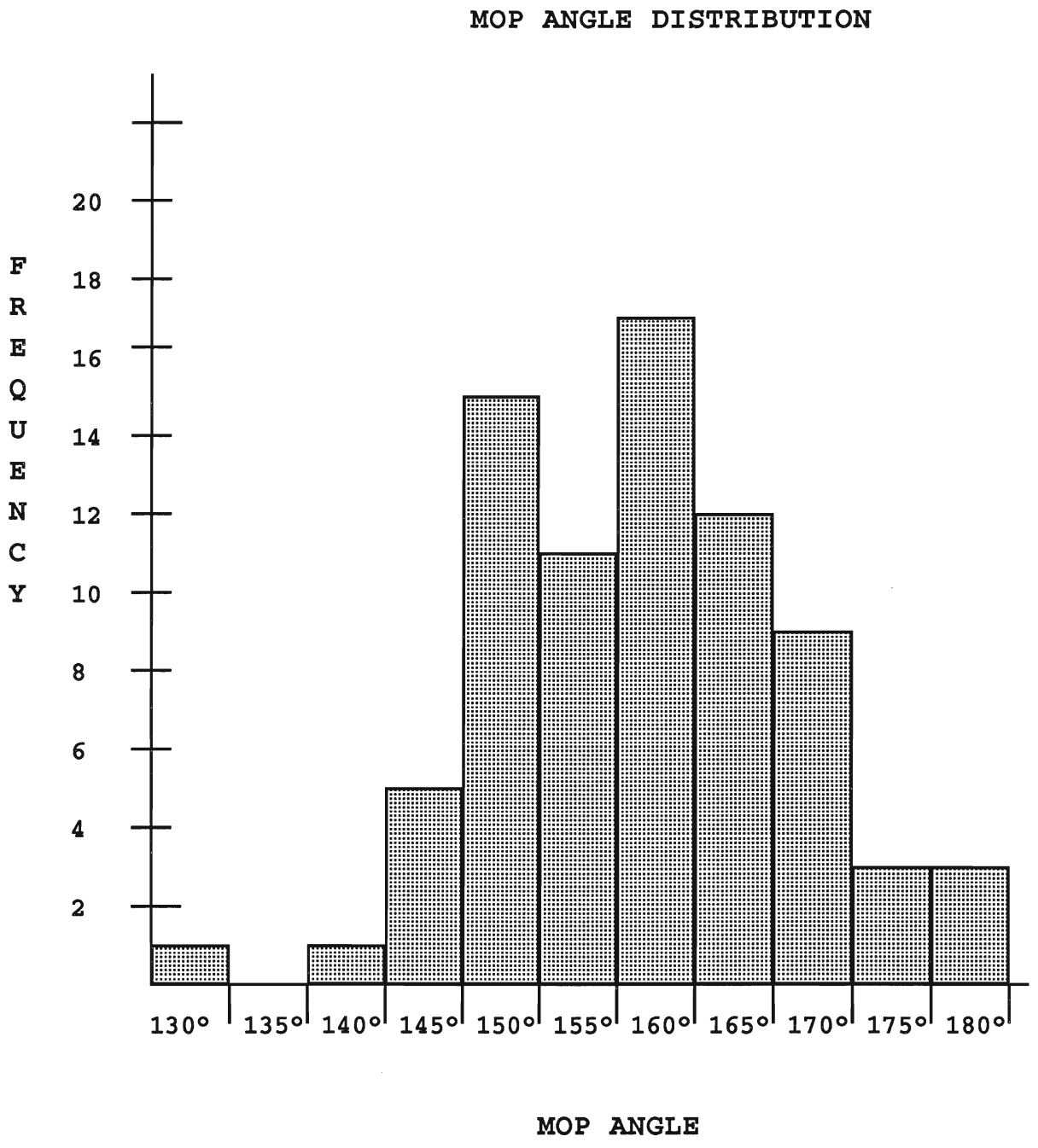

Figure xxiii: ***Distribution of the MOP angle for a group of triphenylphosphineoxide and trialkylphosphineoxide metal complexes.***

this information aside from recognizing the fact that Lewis structures are unequipped to handle these systems. The P-O bond lengths were similarly analyzed with the expectation of finding the O-P bond lengths clustered about values which were near to long O-P values, median O=P values or short O≡P values. There was no evident clustering to suggest the type of bonding between the oxygen and phosphorus.

Many experiments have been performed to try and determine the bonding type and many solutions have been proposed.[31-34] In general, it has been agreed that a combination of sigma and pi bonding occurs.

The origin of the sigma bonding has been established as oxygen p-orbitals interacting with phosphorus p-orbitals. Presumably the lone pair on the PR_3 group is donating to an empty oxygen orbital.

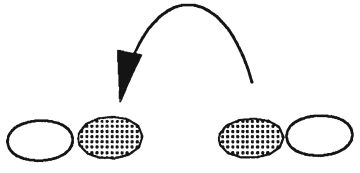

The outer shell s orbital of oxygen is filled and the

remaining oxygen p orbitals are thought to interact with the phosphorus through π interactions.

The origin of the π bonding has proved to be more controversial than the σ interactions. It has been speculated that there is back donation of two electron pairs of oxygen into phosphorus 3d orbitals.[35]

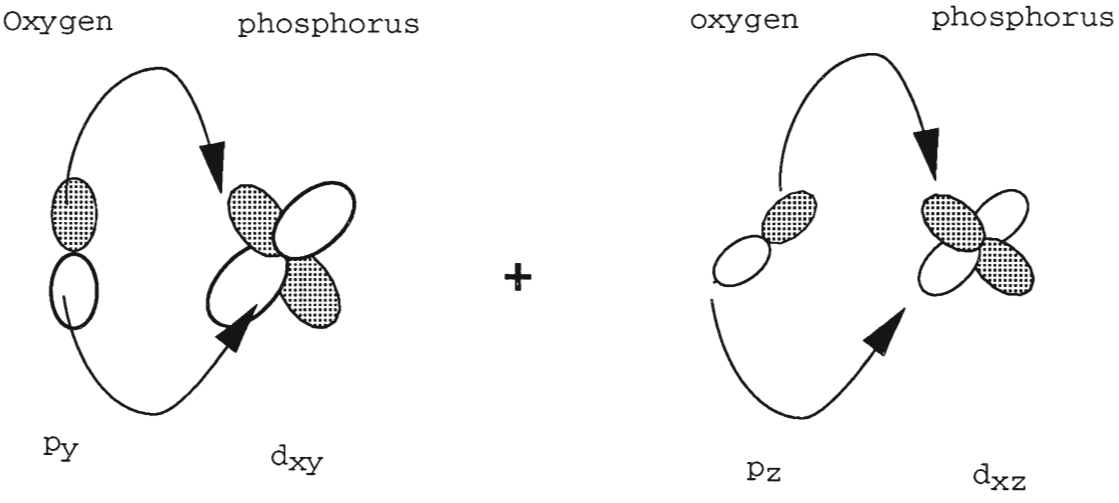

This description readily fits the triple bond assumption. The variation in bond angle also follows, since this type of bonding has poor overlap,[35] and, therefore, lends itself well to an assumption of flexibility about the bond.

Arguments in the literature[36] that the 3d orbitals

of phosphorus are too diffuse to interact have been countered with suggestions that electronegative substituents on phosphorus are able to contract the 3d orbitals.[37] This allows the d orbitals to participate in overlap with the 2p orbitals of oxygen and therefore increase the O-P bond order.

In the last few years many papers have emerged which attempt to omit the phosphorus 3d orbitals entirely.[38,39] A popular idea is that anti-bonding PR_3 molecular orbitals are being utilized as π-electron density acceptors.[38] The phosphorus acceptor molecular orbital is then considered to be almost completely p-orbital in character. Other studies also suggest the role of 3d orbitals is negligible, with molecular orbitals of only 13%-15% d-character.[37] This small contribution has been attributed to shaping the p-orbitals so that they are better able to overlap ligand bonding orbitals.[39]

Despite all of the speculation and the different approaches taken to P-O bond examination, a clear description

of the interactions involved has yet to be established.

ii. Harmonic vs Anharmonic Treatment of the MOP bond angle

If the MOP bond angle was simply assumed to be very flexible, then it follows that electronic and steric properties of nearby groups could easily influence the bond angle. That is, if a low energy barrier is assumed for movement about an equilibrium angle, the variation in the bond angle could be partially explained. There are several options in the molecular mechanics approximation for parameterization of flexibility. One method involves a very low force constant with the MM2 function. Another method varies the actual analytic expression for energy as a function of bond angle.

Initially, various force constants were set with the MM2 function. It was found that decreasing the force constant, k_θ, to an unusually low value provided satisfactory results. From Table ***V*** it can be see that at k_θ = 10 kcal/molrad^2 the MOP angles are larger than when k_θ = 30 kcal/molrad^2. With the smaller force constant the angles are also spread farther

COMPOUND	OBSERVED VALUE		MM2 MINIMIZATION		MM2 MINIMIZATION	
			$k=30,\ \theta_o=140°$		$k=10,\ \theta_o=140°$	
	$SnOP_1$	$SnOP_2$	$SnOP_1$	$SnOP_2$	$SnOP_1$	$SnOP_2$
$SnBr_2Et_2(tppo)_2$	157.8	157.9	152.7	154.0	157.6	160.7
$SnBr_3Et(tppo)_2$	155.3	158.4	152.2	152.3	157.1	160.0
$SnBr_4(tppo)_2$	160.2	151.8	152.6	150.8	159.1	156.7
$SnI_2Et_2(tppo)_2$	150.1	167.2	149.5	152.4	154.0	163.2
$SnI_3Et(tppo)_2$	155.7	159.3	155.7	155.6	160.6	159.0
$SnI_4(tppo)_2$	152.0	161.5	152.6	155.4	158.3	164.7

Table V: ***Comparison of different constants for the MM2 angle terms.*** Angles in degrees. Constants in $(kcal/mol)/rad^2$

apart, even within the same molecule. For example with $SnI_4(tppo)_2$ the MOP angles move from 152.6° and 155.4° to 158.3 and 164.7° as the force constant is decreased. These values compare favorably with the experimental spread of 8.5° (Table V). Although the angles were reproduced better than expected with this approach, inconsistencies still existed and it was suspected that these could be further reduced.

The bond angle functions available were reviewed (equations 5 to 7) and it was concluded that the cosine harmonic function would be suitable due to its non-extreme behavior away from equilibrium. Comparison of the MM2 function and the cosine harmonic function curves (Figure ***xxiv***) indicates that, near the equilibrium value, there is little difference in the behavior of the two. However, at angles which are much larger than the equilibrium value, the two curves diverge and the MM2 function term has significantly higher energy than the cosine harmonic.

Since the metal-phosphine oxide complexes generally have MOP angles which may vary by as much as 50°

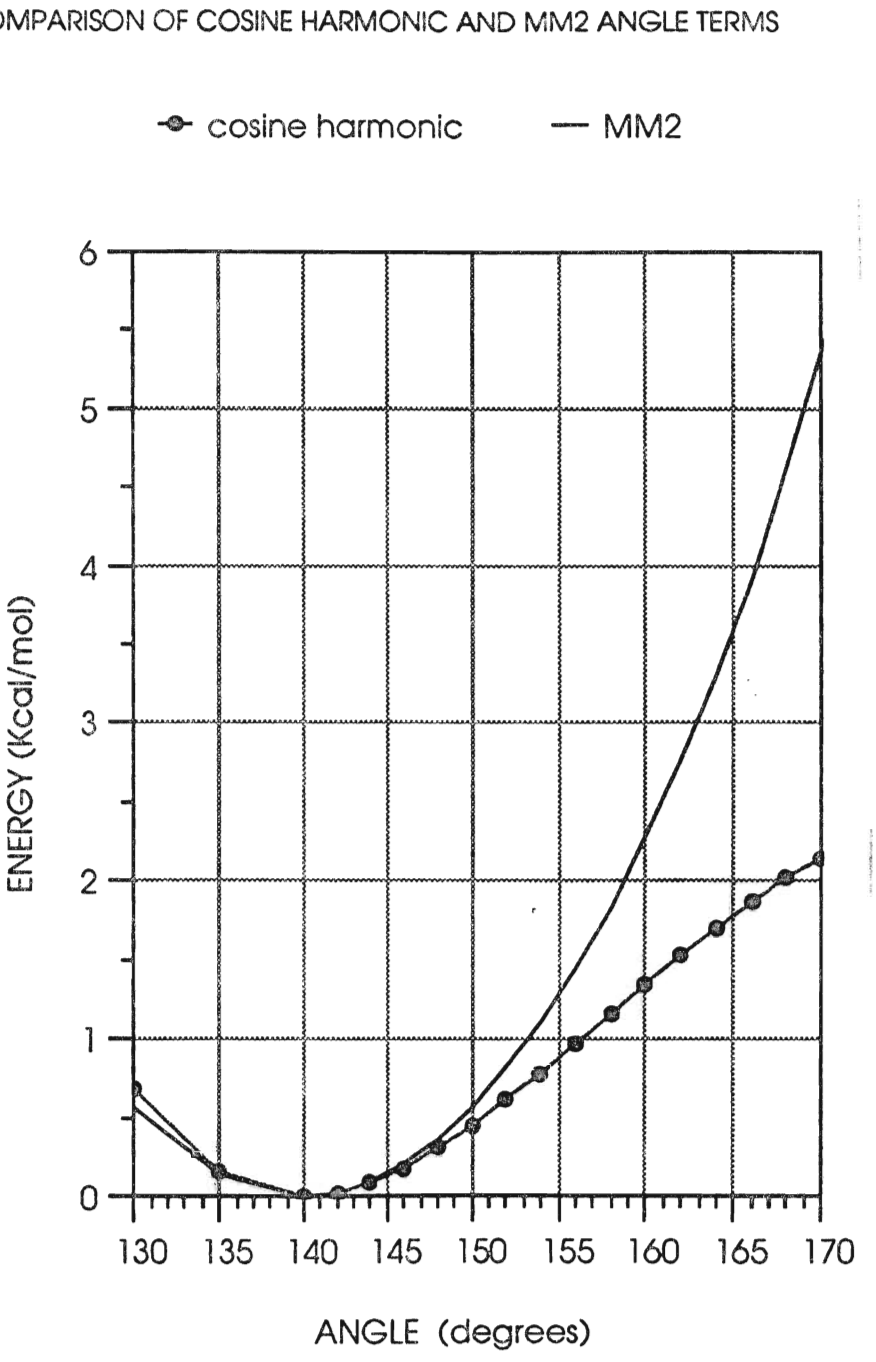

Figure xxiv: ***Comparison of the MM2 and cosine harmonic curves.*** θ_O=140° and k=37 kcal/molrad^2 for MM2 curve and k=37 kcal/mol for the cosine harmonic curve

from one molecule to another and almost 20° within a molecule a large energy component for these angles would not be expected. This suggests that the cosine harmonic function more accurately represents the MOP angle bending since it does not have an unsuitable increase in energy as the angle moves from equilibrium. The change in energy is approximately 2.5 kcal/mol over 30° for the cosine harmonic function compared to 5.5 kcal/mol for the MM2 function.

A comparison of the two functions in terms of the MOP angle can be seen in Table ***VI***. From this Table it would seem that the cosine harmonic term is best able to replicate the disparity of the angles. The MM2 force field tends to keep the angles close to one another at a value similar to that set in the parameters. This is evident from the clustering of the angles around 150°. Clustering does not occur when the harmonic function is used where angles are seen from 150° for $SnI_2Et_2(tppo)_2$ to 166° for $SnI_4(tppo)_2$. The cosine harmonic function also allows a 10° difference between bonds of the same molecule, as in

COMPOUND	OBSERVED VALUE		COSINE HARMONIC MINIMIZATION		MM2 MINIMIZATION	
K=37 θ_o=140°	$SnOP_1$	$SnOP_2$	$SnOP_1$	$SnOP_2$	$SnOP_1$	$SnOP_2$
$SnBr_2Et_2(tppo)_2$	157.8	157.9	153.9	157.4	151.4	152.1
$SnBr_3Et(tppo)_2$	155.3	158.4	155.0	158.0	151.1	151.2
$SnBr_4(tppo)_2$	160.2	151.8	155.4	152.2	151.3	149.6
$SnI_2Et_2(tppo)_2$	150.1	167.2	150.6	160.7	148.6	150.8
$SnI_3Et(tppo)_2$	155.7	159.3	159.4	160.1	151.8	151.1
$SnI_4(tppo)_2$	152.0	161.5	155.1	166.7	151.0	153.3

Table VI: ***Comparison MM2 and cosine harmonic angle terms for*** $SnX_yR_z(tppo)_2$

Angles in degrees. Constants in (kcal/mol)/rad^2 for the MM2 function and in kcal/mol for the cosine harmonic function.

$SnI_4(tppo)_2$.

It is possible to conclude from this information that the cosine harmonic function approximates the energy curve of the MOP angle more closely than does the sextic MM2 function as the angle is moved away from the equilibrium value.

iii. Crystal packing forces

Knowing the exact nature of the O-P bond would help in modeling the structures involved, but this information is not essential. It can be assumed that there does exist a natural value for the MOP angle but that the angle is easily influenced to move from that value. Isolating the interactions responsible for shifting the angle would be useful in determining the capacity of molecular mechanics to duplicate the trend. Crystal packing, van der Waals forces, and the nature of the non-phosphine-oxide ligands may all play important roles in determining which MOP angle exists and are phenomena which may be simulated with molecular

mechanics.

Crystal packing was considered an influence on the MOP bond angle. A large variation in this angle is evident even within structures which appear to contain two equivalent phosphine oxide groups. For example, $SnBr_4(tppo)_2$ would be expected to contain two similar SnOP bond angles since both phosphine oxide ligands appear to have identical environments.

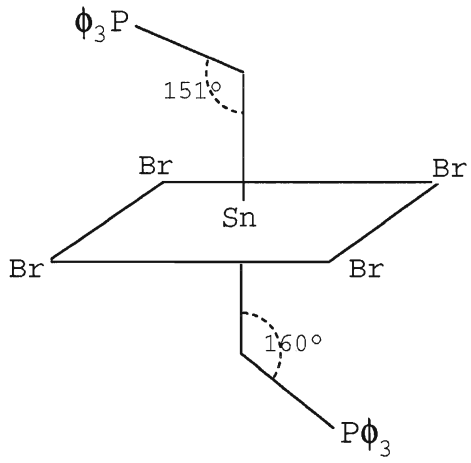

The observed MOP angles are, however, 151° and 160°. The cosine harmonic function was only able to account for 3.2° of the disparity for this molecule. The remaining difference might then be explained by assuming that intermolecular forces are involved. Therefore information about the manner in which molecules assemble with respect to one another in a crystal is needed to test this hypothesis. This information is available from crystallographic data. Using BIOGRAF it is possible to use crystallographic coordinates and space groups to generate the molecules arranged as they would be found in the crystal. By surrounding a central molecule with its nearest neighbors and its next nearest neighbors, it may be possible to recreate the sequence of molecular interactions which lead to crystallization. The central molecule is then surrounded approximately as it would be in the crystal and the geometry of the complex is under the influence of the surrounding particles.

To verify that the first shell contained the most important interactions, a comparison between surrounding the

central molecule with one shell or two shells was made. Addition of the second shell slowed calculation down considerably and did not seem to improve the fit of the MOP angle. It appears therefore that the first shell contains the most important interactions with respect to the MOP angle.

By comparison of geometry after energy calculations of molecules in the "gas" phase and the "solid" phase, some insight may be gained into the extension of molecular mechanics to crystal packing interactions (Table ***VII***).

Minimization of the cluster quite clearly reproduces the SnOP angles more accurately. This is especially true for the trans isomers which should have equivalent intramolecular interactions for both the MOP angles. For the trans-$SnBr_4(tppo)_2$ molecule the error of the SnOP bond angles of the minimized structures without the shell are 4.4° and 8.3°. Surrounding the central molecule

Compound	Observed value		Minimized Single molecule		Minimized Core molecule	
K=37 kcal/mol θ_o=140°	$SnOP_1$	$SnOP_2$	$SnOP_1$	$SnOP_2$	$SnOP_1$	$SnOP_2$
trans $SnBr_4(tppo)_2$	151.8	160.5	155.4	152.2	151.8	159.3
trans $SnCl_3Et(tppo)_2$	148.3	158.3	151.2	153.0	149.3	157.0
cis $SnCl_4(tppo)_2$	157.2	157.2	152.0	152.0	152.0	152.0
cis $SnI_4(tppo)_2$	152.0	163.7	155.2	166.7	154.3	164.4

Table VII: ***The SnOP angle as minimized with and without neighbours.*** Cis/trans designation refers to triphenylphosphine oxide groups.

improves the error to just greater than 1° in the worst case. This is a significant improvement in the angle. From Table ***VII*** it is also evident that the cis isomers seem less susceptible to crystal packing forces than are the trans isomers. For cis-$SnI_4(tppo)_2$ the average error of the single molecule is 3° whereas the average error of the packed molecule is 1.5°.

Although minimization of the cis isomers with the shell around the central molecule does improve the MOP angle somewhat, the difference is not as pronounced as with the trans isomers. This difference in packing dependence suggests one reason for the variation in SnOP angles in these compounds. With both isomers it seems that the phenyl groups of the triphenylphosphine oxides interact with one another and these interactions are quite influential in determining the SnOP bond angles that form. Based on the dependence of SnOP on crystal packing it can be said that the phenyl groups of trans isomers interact with intermolecular phenyl groups

strongly, whereas for the cis isomers the tppo ligands tend to interact with intramolecular phenyl groups. It seems the cis configuration places these groups within a radius which facilitates intramolecular involvement, more so than the trans isomer. This can be seen quite clearly in Figures ***vii-xiv.***

For cis-$SnCl_4(tppo)_2$ molecular mechanics could not duplicate the SnOP angle regardless of the packing attempted. This may signify that the forces which influence the bond angle so that it is 157.2° are electronic in nature or, may simply be a result of a function which is not properly representative of the energy interactions.

Since crystal packing of the triphenylphosphine oxides improved the overall accuracy of the SnOP bond angle fit it was decided to conduct all remaining experiments under crystal packed conditions.

B. MM and the Sn-halogen bond lengths

Initial molecular mechanics minimization with standard parameters revealed that, in general, the experimental values for tin halogen bond lengths (Table ***VIII***) could not be consistently reproduced. Two approaches were taken in order to optimize the molecular mechanics results. The first method varied the constants of Allinger's cubic function, k and d.

$$E = \frac{1}{2} k [(r-r_o)^2 + d(r-r_o)^3] \qquad [7]$$

The cubic term in this function allows for anharmonicity, and follows from the concept that it is more difficult to compress a bond than to stretch it from the equilibrium value. By making use of k and d, an attempt was made to produce a curve with a fairly gradual slope and a wide range of low energy as r moved form r_o (Figure ***xxv***). It was hoped that this would allow the tin halogen distance to fall near the experimental value without a high cost in energy.

From Table ***IX*** it can be seen that even with a low force constant it was not possible to fit the observed values

COMPOUND	Sn-Cl1	Sn-Cl2	Sn-Cl3	Sn-Cl4
trans-$Cl_3Et(tppo)_2$	2.487	2.498	2.360	
cis-$SnCl_4(tppo)_2$	2.386	2.390	2.379	2.387
	Sn-Br1	**Sn-Br2**	**Sn-Br3**	**Sn-Br4**
trans-$SnBr_3Et(tppo)_2$	2.654	2.652	2.504	
trans-$SnBr_4(tppo)_2$	2.511	2.584	2.576	2.558
	Sn-I1	**Sn-I2**	**Sn-I3**	**Sn-I4**
trans-$SnI_2Et_2(tppo)_2$	2.916	3.127		
trans-$SnI_3Et(tppo)_2$	2.895	2.957	2.723	
cis-$SnI_4(tppo)_2$	2.835	2.712	2.654	2.951

Table VIII: ***Experimental tin-halogen bond lengths.***
Tin halogen bond lengths, in angstroms.
Cis/trans designation for the compound name refers to tppo groups.

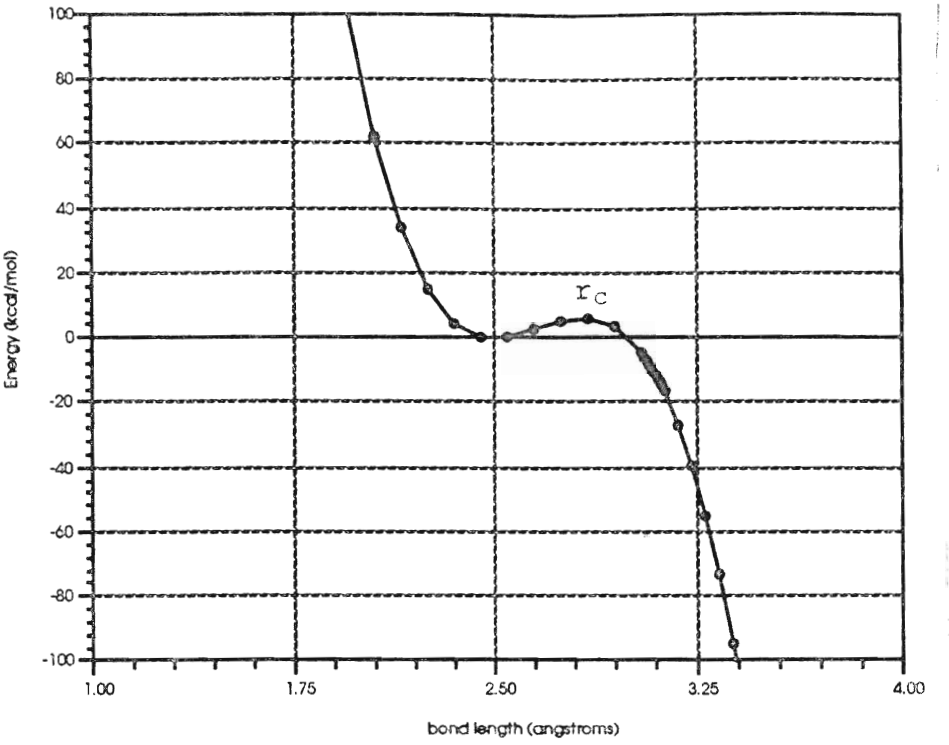

Figure xxv: ***Cubic potential energy function.*** Cubic has k=323kcal/molÅ², d=-2 kcal/molÅ and r_o=2.5Å

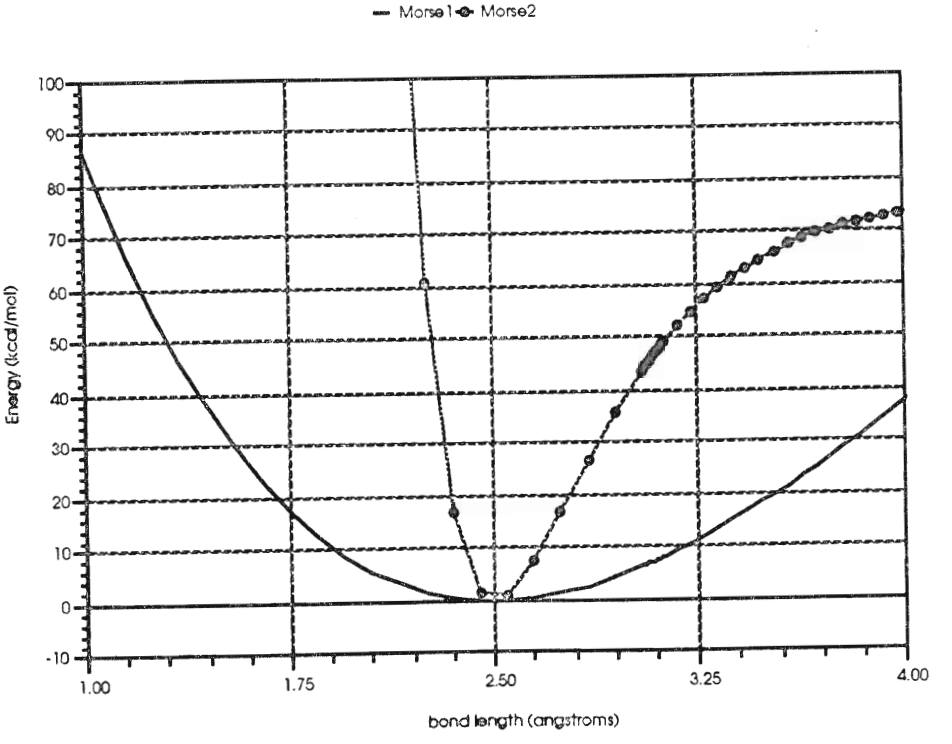

Figure xxvi: ***Morse potential energy function.*** Morse1 has k=50 kcal/molÅ, D=323 kcal/mol and r_o=2.5Å.
Morse2 has k=100 kcal/molÅ D=77 kcal/mol and r_o=2.5Å

SOURCE	k	D or d	Sn-Cl1	Sn-Cl2	Sn-Cl3
OBSERVED			2.487Å	2.498Å	2.360Å
MORSE FUNCTION	5	80	2.370Å	2.500Å	2.368Å
	15	77	2.459Å	2.512Å	2.372Å
	100	0.5	2.399Å	2.407Å	2.398Å
	1000	0.1	2.399Å	2.971Å	2.459Å
CUBIC FUNCTION	10	-2	2.467Å	2.507Å	2.379Å
	320	-2	2.400Å	2.403Å	2.400Å
	320	-5.5	2.400Å	2.403Å	2.399Å
	500	-5.5	2.400Å	2.400Å	2.399Å
	1200	-5.5	2.400Å	2.400Å	2.400Å

Table IX: ***Comparison of the Morse and cubic functions for the trans-$SnCl_3Et(tppo)_2$ molecule.***

r_o=2.40Å, k is in kcal/molÅ^2, D is in kcal/mol and d is in kcal/molÅ

accurately. The low force constant introduced difficulties with respect to the nature of the cubic curve. From Figure ***xxv*** it can be seen that, if a bond length is greater than a critical value, r_c, the molecule would fly apart, since the energy continually improves as the bond length increases. With a low k value it is considerably easier to reach r_c and subsequently dissociate the molecule. Although BIOGRAF has compensated for long bond lengths by changing the sign of the cubic term, the behavior of the this curve past r_c does not correlate with the observed behavior nor does it match other popular functions. In order to reduce the risk of overstepping r_c, many d values were tried in combination with several k values. By changing the value of d and k it was possible to modify the bond distance at which the maximum occurred as well as the height of the maximum. Although altering d changed the location of the maximum, the fit of the Sn-X was not improved.

Another option available with BIOGRAF is the use of a Morse potential (eq 6) to calculate bond energy. Since

this function mimics the behavior of a real bond more closely than does the MM2 function several analyses were conducted.

$$E = D\{\exp[-(k/2D)^{1/2}(r-r_o)] - 1\}^2 \qquad [6]$$

In this case D represents the dissociation energy and k is again the force constant (Figure ***xxvi***). Since the dissociation energies of tin-halogen bonds are known, these values can be used as starting points for D. We are left with modifying k, which is again assumed to be low as a consequence of a flexible bond. The use of the Morse function did improve the accuracy of the results somewhat, however, more importantly, trends in the differences in bond length were slightly better reproduced with the Morse function. It can be see from Tables ***X*** and ***XI*** that for the three $SnX_3Et(tppo)_2$ groups, the Sn-X3 bond length was approximately 0.01Å shorter when the Morse function was used than when the cubic function was used. Although the accuracy is not markedly increased with the Morse function it was thought worth while to maintain this term for what improvement it could afford and the assurance of a well

COMPOUND	cubic variables	Sn-X1	Sn-X2	Sn-X3	Sn-X4
trans-$Cl_3Et(tppo)_2$	K=10kcal/molÅ^2 r_o=2.55Å d=-2kcal/molÅ	2.467	2.507	2.379	
cis-$SnCl_4(tppo)_2$		2.412	2.450	2.411	2.451
trans-$SnBr_3Et(tppo)_2$	K=15kcal/molÅ^2 r_o=2.67Å d=-2kcal/molÅ	2.666	2.629	2.585	
trans-$SnBr_4(tppo)_2$		2.600	2.530	2.488	2.587
trans-$SnI_2Et_2(tppo)_2$	K=15kcal/molÅ^2 r_o=2.90Å d=-2kcal/molÅ	2.869	3.268		
trans-$SnI_3Et(tppo)_2$		2.830	2.967	2.817	
cis-$SnI_4(tppo)_2$		2.917	2.844	2.827	2.857

Table X: ***Tin halogen bond lengths, (Å), obtained by minimization with the cubic stretching function.***

COMPOUND	morse variables	Sn-X1	Sn-X2	Sn-X3	Sn-X4
trans-$Cl_3Et(tppo)_2$	K=10kcal/mol$Å^2$ r_o=2.55Å D=77kcal/mol	2.459	2.512	2.372	
cis-$SnCl_4(tppo)_2$		2.346	2.411	2.420	2.511
trans-$SnBr_3Et(tppo)_2$	K=15kcal/mol$Å^2$ r_o=2.67Å D=65kcal/mol	2.668	2.624	2.573	
trans-$SnBr_4(tppo)_2$		2.607	2.489	2.461	2.593
trans-$SnI_2Et_2(tppo)_2$	K=15kcal/mol$Å^2$ r_o=2.90Å D=50kcal/mol	2.849	3.034		
trans-$SnI_3Et(tppo)_2$		2.826	2.947	2.794	
cis-$SnI_4(tppo)_2$		2.909	2.834	2.815	2.845

Table XI: ***Tin halogen bond lengths, (Å), obtained by minimization with the Morse stretching function.***

behaved curve at all values of r.

From Tables ***X*** and ***XI*** it can also be seen that fairly low stretching constants were used for the tin halogen bonds. In order to substantiate these low values some rough calculations were conducted. Vibrational spectra of octahedrally coordinated tin were found.[40] The two modes associated with stretch motion from the spectra of $[SnCl_6]^{2-}$, $[SnBr_6]^{2-}$, and $[SnI_6]^{2-}$ were isolated. These modes were assumed to be independent of any other vibrational motion. That is, since the O-H stretch in complex hydroxy containing molecules and in the hydroxy radical occur at a similar frequency similar circumstances were predicted for tin complexes. Thus a simple calculation was possible using equation [17].

$$k=(2\pi c\upsilon)^2\mu \qquad [17]$$

where $c=3X10^8 m/s$, υ is the wave number in cm^{-1}, and μ is the reduced mass. The result of these calculations can be seen in Table ***XII.***

The constants thus generated for tin-chlorine,

tin-bromine, and tin-iodine were of the same order of magnitude as those approximated for the molecular mechanics energy experiments. Although the two sets of stretch constants are not identical, they are similar enough to justify the use of stretching constants which are very small, that is, less than a tenth of the value typical for C-C bonds (Table ***II***).

After many unsuccessful attempts at consistently reproducing the Sn-X bond lengths some experiments were done to test the magnitude of the steric influence on these bonds. $SnCl_3Et(tppo)_2$ was chosen as a test molecule in a set of experiments which maintained a fairly low Morse stretch

Halogen	υ_{Sn-X}	force constant from equation 17	force constant used in minimizat^n
Chlorine	160 (cm^{-1})	60 (kcal/mol)	10 (kcal/mol)
Bromine	80 (cm^{-1})	25 (kcal/mol)	15 (kcal/mol)
Iodine	50 (cm^{-1})	13 (kcal/mol)	15 (kcal/mol)

Table XII: ***Stretch constants.***

constant of 100kcal/mol$Å^2$ and varied r_o from 2.30Å to 2.50Å. These experiments revealed that, regardless of the strain-free value chosen, the minimized structure contained three equivalent Sn-Cl bond lengths which were all within 0.01Å of the strain-free value selected. This indicates that steric factors are not principle in determining the Sn-X bond length. To completely eliminate steric interactions all non-halogen atoms were frozen during a minimization. These experiments revealed that when low r_o values are selected, (i.e., <2.4Å) similar results are obtained as when all atoms were allowed to optimize. However, at longer strain-free values one or more of the halogens began to infringe on the van der Waal radii of the phenyl systems. Therefore steric influences could not be disregarded as an influence on the Sn-X bond length. With this information it is possible to visualize a number of interactions that includes some steric involvement but which are most likely compounded by electronic effects which may include the trans effect[41] and cis weakening.[17-25]

There exists no direct approach with molecular mechanics for simulation of electronic effects. Indirectly it is possible to parameterize all cis and trans groups separately. That is, all groups cis to a donor would be parameterized with different strain free values than their trans counterparts. This system may improve the fit of the molecules, however, there would be a substantial increase in the time required for parameterization.

C. MM and the Sn-O, Sn-C, O-P and P-C bond lengths

The Sn-O, Sn-C, O-P and P-C bond lengths were better parameterized than the Sn-X bond lengths in most cases. Tables ***XIII*** and ***XIV*** present the observed values and those values obtained with MM energy minimization using the parameters listed in Tables ***II, III*** and ***IV.*** The Sn-O and Sn-C bond lengths may also be influenced by the trans and cis donors and, as such, their bond lengths were not fit as closely as would have been hoped. Although not as poorly reproduced as the Sn-X bonds similar experiments as in the halogen case were attempted. These experiments failed to

Molecule	Sn-O		Sn-C		O-P		P-C		
trans-Cl_3Et $(tppo)_2$	2.18	2.17	2.13		1.52	1.52	1.79	1.78	1.79
							1.78	1.81	1.79
cis-$SnCl_4$ $(tppo)_2$	2.08	2.08			1.51	1.51	1.79	1.79	1.80
							1.79	1.79	1.80
trans-$SnBr_3Et$ $(tppo)_2$	2.21	2.21	2.26		1.52	1.54	1.80	1.76	1.76
							1.68	1.81	1.79
trans-$SnBr_4$ $(tppo)_2$	2.10	2.10			1.50	1.53	1.80	1.81	1.80
							1.81	1.80	1.80
trans-SnI_2Et_2 $(tppo)_2$	2.25	2.29	2.29	2.04	1.50	1.49	1.80	1.80	1.78
							1.79	1.80	1.79
trans-SnI_3Et $(tppo)_2$	2.25	2.21	2.25		1.49	1.51	1.78	1.81	1.80
							1.80	1.82	1.83
cis-SnI_4 $(tppo)_2$	2.26	2.08			1.47	1.50	1.84	1.79	1.77
							1.80	1.78	1.81

Table XIII: ***Observed Sn-L bond lengths,(in Å),as obtained from crystal data.***

Molecule	Sn-O		Sn-C		O-P		P-C		
trans-Cl_3Et $(tppo)_2$	2.19	2.18	2.16		1.52	1.51	1.80	1.79	1.80
							1.79	1.79	1.80
cis-$SnCl_4$ $(tppo)_2$	2.17	2.17			1.51	1.51	1.79	1.79	1.79
							1.79	1.79	1.79
trans-$SnBr_3Et$ $(tppo)_2$	2.23	2.30	2.20		1.50	1.53	1.79	1.80	1.80
							1.79	1.78	1.80
trans-$SnBr_4$ $(tppo)_2$	2.17	2.16			1.51	1.50	1.80	1.79	1.79
							1.79	1.80	1.80
trans-SnI_2Et_2 $(tppo)_2$	2.19	2.21	2.18	2.16	1.52	1.53	1.80	1.79	1.80
							1.80	1.79	1.80
trans-SnI_3Et $(tppo)_2$	2.19	2.16	2.17		1.53	1.52	1.79	1.80	1.80
							1.80	1.80	1.80
cis-SnI_4 $(tppo)_2$	2.17	2.16			1.51	1.50	1.80	1.80	1.80
							1.79	1.80	1.79

Table XIV: ***Bond lengths, in Å, after minimization with parameters listed in table II.***

reduce the error and a cubic function with unremarkable force constants was used in the final calculation.

D. MM and the SnOPC torsion angles

A cursory glance at Table ***XV*** seems to imply that the SnOPC torsion angles are not well reproduced with the parameters selected. However by correlating the torsion angle to the SnOP angle (Figure ***xxvii***) it can be seen that the error in the torsion increases as the MOP angle approaches 180°. At an MOP angle of 180° the torsion angle has no meaning and at MOP values in the range of 160° and 180° the significance of the torsion angle declines as does the significance of the error in the reproduction of those angles. Given that the torsion force constants were set to nearly zero it was thought that these angles were reproduced quite well by simply allowing van der Waals interactions to dominate.

molecule	SnOPC_R	Φ_{obsvd}	Φ_{min}	SnOPC_R	Φ_{obsvd}	Φ_{min}
trans-Sn Cl_3Et $(tppo)_2$	SnO1P1C_R1	-167.6	167.7	SnO2P2C_R1	5.0	2.3
	SnO1P1C_R2	-51.2	-50.6	SnO2P2C_R2	124.3	122.5
	SnO1P1C_R3	73.7	72.4	SnO2P2C_R3	-118.7	-122.6
cis-Sn Cl_4 $(tppo)_2$	SnO1P1C_R1	-155.7	-153.9	SnO2P2C_R1	-154.8	-159.0
	SnO1P1C_R2	84.3	85.8	SnO2P2C_R2	85.3	80.7
	SnO1P1C_R3	-36.4	-34.6	SnO2P2C_R3	-35.5	-40.0
trans-Sn Br_3Et $(tppo)_2$	SnO1P1C_R1	-48.3	-50.6	SnO2P2C_R1	26.6	-11.07
	SnO1P1C_R2	-165.3	-166.6	SnO2P2C_R2	144.1	132.7
	SnO1P1C_R3	72.9	73.8	SnO2P2C_R3	-98.7	-110.1
trans-Sn Br_4 $(tppo)_2$	SnO1P1C_R1	152.7	-151.3	SnO2P2C_R1	85.4	83.1
	SnO1P1C_R2	-33.5	-33.1	SnO2P2C_R2	-158.0	-162.5
	SnO1P1C_R3	100.7	89.4	SnO2P2C_R3	38.7	41.2
trans-Sn I_2Et_2 $(tppo)_2$	SnO1P1C_R1	108.5	101.6	SnO2P2C_R1	55.4	123.1
	SnO1P1C_R2	-133.7	-139.7	SnO2P2C_R2	174.3	-117.9
	SnO1P1C_R3	-11.9	-19.9	SnO2P2C_R3	-68.1	-0.2
trans-Sn I_3Et $(tppo)_2$	SnO1P1C_R1	-7.2	-17.1	SnO2P2C_R1	71.48	80.2
	SnO1P1C_R2	114.2	104.1	SnO2P2C_R2	-168.4	-159.7
	SnO1P1C_R3	129.6	-137.1	SnO2P2C_R3	-53.1	-44.2
cis-Sn I_4 $(tppo)_2$	SnO1P1C_R1	-35.7	-50.9	SnO2P2C_R1	28.8	51.7
	SnO1P1C_R2	88.8	75.1	SnO2P2C_R2	144.7	167.3
	SnO1P1C_R3	-153.9	-171.6	SnO2P2C_R3	-95.4	-71.2

Table XV: ***Comparison of the more important torsion angles before, Φ_{obsvd}, and after, Φ_{min}, minimization.***

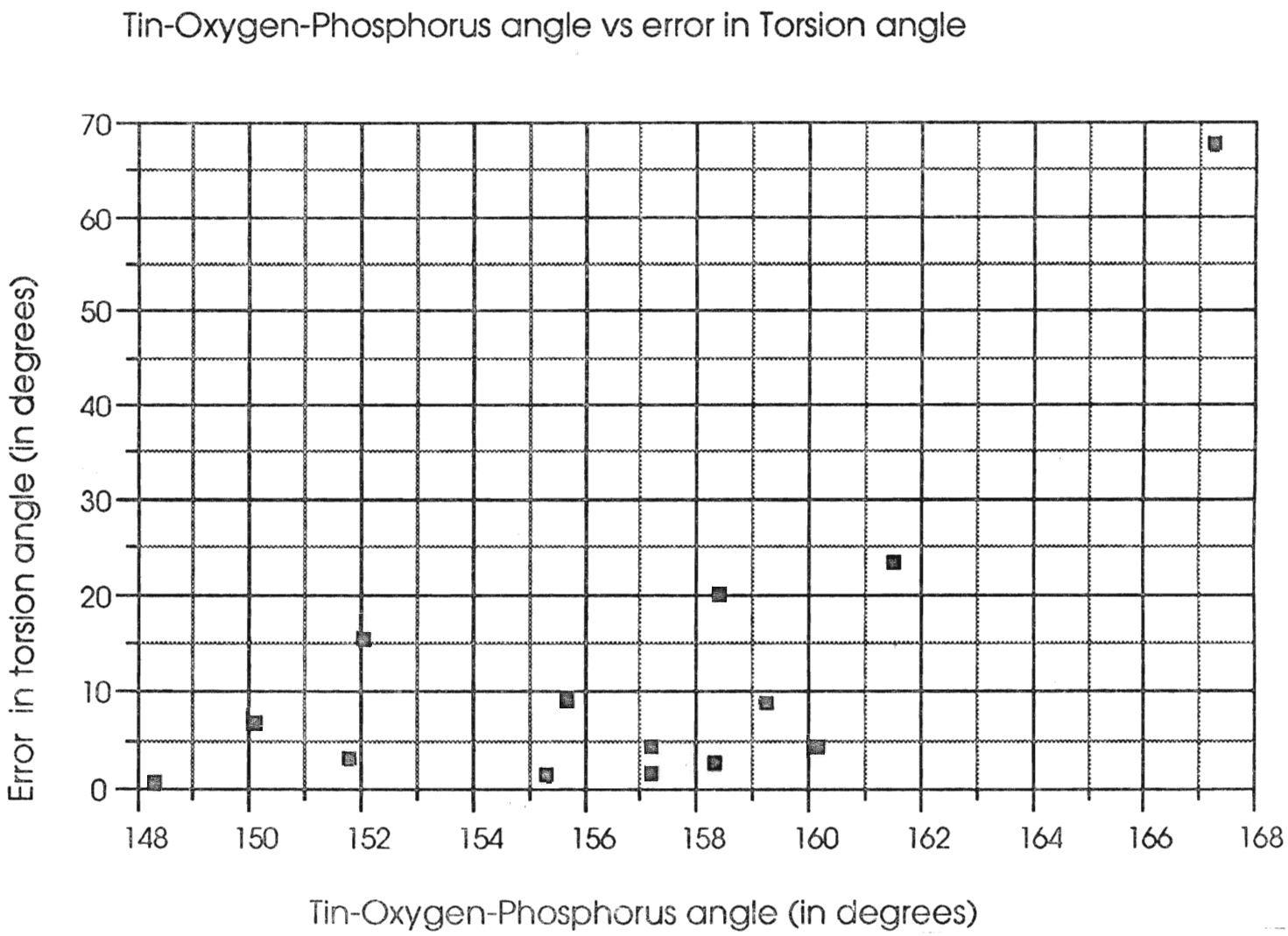

Figure xxvii: ***Torsion angle vs Sn-O-P angle***

E. MM and the halogen-Sn-halogen bond angles

The observed angles about the tin were near 90° as expected for octahedral coordination. (Table **XVI**). The observed values were well reproduced by molecular mechanics in most cases with the exception of the I3SnI2 and the O2SnO1 angles of cis-$SnI_4(tppo)_2$. The observed values were 102.2° and 78.8° which are the two most extreme values of the set of XSnX bond angles. Even though the molecular mechanics values are not within an acceptable margin of error, the experimental I3SnI2 value was 94.6° which was among the highest values reproduced and the experimental O2SnO1 was 85.7° which was the lowest value reproduced. Although the fit of these angles was not as close as would have been desired, the shift of the angles away from 90° was in the correct direction.

Since the angles involved in octahedral coordination were fit accurately, it seems that ignoring all angles of 180°, and treating specifically only the 90° angles does not have adverse effects on the molecular mechanics treatment of the angles about tin.

molecule	X Sn X	θ_{obsvd}	θ_{min}	X Sn X	θ_{obsvd}	θ_{min}	X Sn X	θ_{obsvd}	θ_{min}
trans-Sn Cl_3Et $(tppo)_2$	Cl3SnCl1	86.8	87.1	Cl3SnCl2	88.1	89.2	Cl1SnO1	90.4	89.9
	Cl2SnO1	90.9	90.3	Cl3SnO1	89.6	89.8	Cl1SnO2	90.9	90.6
	Cl2SnO2	87.9	89.3	Cl3SnO2	90.9	91.4	Cl1SnC1	95.0	94.7
	Cl2SnC1	90.1	89.0	O1SnC1	90.1	89.7	O2SnC1	89.3	89.0
cis-Sn Cl_4 $(tppo)_2$	Cl2SnCl1	91.0	87.5	Cl1SnO1	86.9	90.5	Cl3SnCl2	95.5	92.2
	Cl3SnO1	86.3	89.8	Cl4SnCl1	95.4	92.9	Cl4SnCl2	91.9	88.7
	Cl4SnO1	90.9	92.3	Cl3SnCl3	91.3	86.9	Cl1SnO2	85.9	90.1
	Cl2SnO2	90.9	89.9	O2SnO1	86.3	89.2	Cl3SnO2	87.1	90.0
trans-Sn Br_3Et $(tppo)_2$	Br3SnBr1	88.0	92.7	Br3SnBr2	88.6	87.9	Br1SnO1	91.1	92.6
	Br2SnO1	89.5	86.9	Br3SnO1	88.2	89.3	Br1SnO2	95.8	89.4
	Br2SnO2	83.7	90.6	Br3SnO2	92.8	93.5	Br1SnC1	88.2	89.0
	Br2SnC1	95.2	92.3	O1SnC1	89.3	88.6	O2SnC1	90.1	87.4
trans-Sn Br_4 $(tppo)_2$	Br3SnBr1	91.3	86.4	Br3SnBr2	88.2	88.6	Br4SnBr1	91.6	88.8
	Br4SnBr2	89.0	89.9	BrSnO1	89.9	89.8	Br2SnO1	87.5	91.8
	Br3SnO1	91.4	89.7	Br4SnO1	91.8	92.4	Br1SnO2	94.5	95.6
	Br2SnO2	88.1	89.3	Br3SnO2	86.26	89.0	Br4SnO2	90.3	88.8
trans-Sn I_2Et_2 $(tppo)_2$	I1SnO1	87.4	92.3	I2SnO1	90.8	88.4	I1SnO2	87.1	90.2
	I2SnO2	93.8	89.2	I1SnC1	91.1	90.4	I2SnC1	83.6	88.0
	O1SnC1	85.8	92.2	O2SnC1	84.2	92.1	I1SnC3	96.5	93.4
	I2SnC3	88.2	88.2	O1SnC3	96.1	85.6	O2SnC3	94.5	89.9
trans-Sn I_3Et $(tppo)_2$	I3SnI1	91.9	89.5	I3SnI2	86.2	85.9	I1SnC1	89.1	89.3
	I2SnC1	92.7	95.3	I1SnO1	87.2	89.9	I2SnO1	92.6	91.0
	I3SnO1	95.1	92.5	O1SnC1	85.2	88.8	I1SnO2	88.6	90.0
	I2SnO2	91.8	89.4	I3SnO2	89.0	89.9	O2SnC1	90.8	89.9
cis-Sn I_4 $(tppo)_2$	I2SnI1	98.2	93.3	I3SnI1	92.4	89.4	I3SnI2	102.2	94.6
	I4SnI1	88.2	89.4	I4SnI2	89.2	87.2	I1SnO1	90.9	92.4
	I3SnO1	86.5	88.4	I4SnO1	81.8	89.9	I2SnO2	91.3	88.6
	I3SnO2	91.1	90.7	I4SnO2	86.2	90.4	O2SnO1	78.8	85.7

Table XVI: ***Angles about the tin as aquired from crystal data, θ_{obsvd}, and as produced after minimization, θ_{min} .***

All angles in degrees.

IV. CONCLUSION

It was initially predicted that some of the tin-halogen bond lengths as well as the tin-oxygen-phosphorus bond angles would be difficult to reproduce. This, in fact, was the case, but a combination of new force constants, variable potential stretching and bending functions, as well as the crystal packing of the molecules of interest provided results which were better than expected.

There can be some confidence now that the structures of these molecules may be well reproduced. It is a leap of faith to assume that a similar accuracy can be expected with the steric energy predictions since no basis for comparison exists. However, the steric energies of the minimized molecules are presented in Table ***XVII.*** The individual energies are not directly comparable since no two molecules have the same composition, however, some observations can be noted.

One observation corresponds to the general agreement between the magnitude of the steric energies for all the

	E_{total}	$E_{stretch}$	E_{bend}	$E_{torsion}$	E_{VDW}
trans-$SnCl_3Et$ $(tppo)_2$	-29.003	4.248	3.993	-58.514	21.270
cis-Sn Cl_4 $(tppo)_2$	-35.925	4.301	2.531	-58.972	16.215
trans-$SnBr_3Et$ $(tppo)_2$	-30.232	3.987	4.418	-58.758	20.030
trans-$SnBr_4$ $(tppo)_2$	-31.720	4.453	4.169	-58.606	18.264
trans-SnI_2Et_2 $(tppo)_2$	-30.349	4.623	5.001	-58.757	18.784
trans-SnI_3Et $(tppo)_2$	-32.539	4.543	4.982	-59.046	16.982
cis-SnI_4 $(tppo)_2$	-36.138	3.944	5.048	-58.434	13.304

Table XVII: ***Steric energies of the isolated core as aquired with the use of the parameters listed in Tables II-IV and crystal packing.***
All energies in kcal/mol.

complexes analyzed. Since the group of compounds are very similar in their substituents as well as the arrangement of the substituents this seems to be a fair indication that the forcefield is consistent.

Having noted the similarity in the list of energies the differences can also be examined. Table ***XVII*** illustrates that the two molecules with cis configuration, cis-$SnCl_4(tppo)_2$ and cis-$SnI_4(tppo)_2$, have lower steric energy than do the trans complexes. Since it is the van der Waals component which improves the steric energies of these molecules, the earlier hypothesis that cis systems have greater intramolecular phenyl ring interactions than the trans systems can be justified.

Armed with good geometric correlation as well as some energy information, it is now possible to continue the experiment. The next step is to proceed to solvation of the metal phosphine oxide complexes in the fulfillment of the original goal: predicting relative energies of various metal, phosphine oxide, and solvent systems.

V. REFERENCES

1. Kendrick, M., May, M., Plishka, M., Robinson, K., *Metals in Biological Systems*, Ellis Harwood, NY, 1992.

2. Kushner, D., *Water Poll. Res. J. Canada*, **1993**, *28*, 111-128.

3. Ravera, O., *Ecological Assesment of Environmental Degradation, Polution and Recovery*. Elsevier Science Publishing Company,Inc. NY. 1989.

4. Doyle, F., Duyvesteyn, S., *JOM*, **1993**, *1*, 46-54.

5. Tait, B., *Solvent Extraction and Ion Exchange*, **1992**, *10*, 799-809.

6. Swaddle, T., *Applied Inorganic Chemistry*. University of Calgary press, 1990, Calgary Alberta, 240-247.

7. Cyanex 921 Solvent Extraction Reagent, *American Cyanamid Company, Technical Report No. SPT 029*.

8. Mwakapumba, J., *Molecular Mechanics Calculations on Some Phosphine Oxide Metal Complexes in Aqueous and Organic Solvents*. A thesis submitted to the Department of Chemistry, Brock University, St.Catharines, Ontario, 1991.

9. Burkert, U., Allinger, N., *Molecular Mechanics*. American Chemical Society, Washington D.C., 1982.

10. Hendrickson, J., *J. Am. Chem. Soc.* **1961**, *83*, 4537.

11. Cambridge Scientific Computing, Inc. 875 Massachusetts Ave.,

Suite 41, Cambridge, MA, Box 021339.

12. Molecular Simulations, Inc. 200 Fifth Ave, Waltham, MA, Box 01254.

13. Rappé, A.K., Casewit, C.J., Colwell, K.S., Goddard, A.W.,Skiff, W.M., *J. Am. Chem. Soc.* **1992**, *114*, 10024-10035.

14. Hay, P., *Coord. Chem. Reviews*. **1993**, *126*, 177-236.

15. Halgren, T.A., *J. Am. Chem. Soc.* **1992**, *114*, 7827-7843

16. Mayo, S. L., Olafson, B. D., Goddard, W. A., *J. Phys. Chem,* **1990,** *94*, 8897-8909.

17. Tursina, A., Alanov, A., Chernyshev, V., Medvedev, S., Yatsenko, A., *Koord. Khim.*, **1985**, *11*, 3753.

18. Tursina, A., Alanov, A., Chernyshev, V., Medvedev, S., Yatsenko, A., *Koord. Khim.*, **1985**, *11*, 1420.

19. Tursina, A., Alanov, A., Chernyshev, V., Medvedev, S., Yatsenko, A., *Koord. Khim.*, **1985**, *11*, 417.

20. Tursina, A., Alanov, A., Chernyshev, V., Medvedev, S., Yatsenko, A., *Koord. Khim.*, **1985**, *11*, 417.

21. Tursina, A., Aslanov, A., Medvedev, S., Yatsenko, A., *Zh. Strukt. Khim.*, **1987**, *28*, 90-92.

22. Tursina, A., Aslanov, A., Chernyshev, V., Medvedev, S., Yatsenko, A., *Zh. Strukt. Khim*, **1986**, *27*, 157.

23. Tursina, A., Alanov, A., Chernyshev, V., Medvedev, S.,

Yatsenko, A., *Koord. Khim.*, **1985**, *11*, 696-701.

24. Tursina, A., Alanov, A., Chernyshev, V., Medvedev, S., Yatsenko, A., *Koord. Khim.*, **1986**, *12*, 420.

25. Tursina, A., Alanov, A., Chernyshev, V., Medvedev, S., Yatsenko, A., *Koord. Khim.*, **1986**, *12*, 420.

26. Hancock, R., *Prog. Inorg. Chem.*, **1990**, *37*, 187-291.

27. Allen, F., Kennard, O., Taylor, R., *Acc. Chem. Res.* **1983**, *16*, 146.

28. Allinger, L. N., *J. Am. Chem. Soc.*, **1977**, *99*, 8127-8134.

29. Liljefors, T., Tai, C., Allinger, N.L., *J. Comput. Chem.*, **1987**, *8*, 1051-1056.

30. Yoshikawa, Y., *J. Comput. Chem.*, **1990**, *11*, 326-335.

31. Marynick, S. D., *J. Am. Chem. Soc.* **1984**, *106*, 4064-4065.

32. Streitwieser, A., Rajca, A., McDowell, R., Glaser, R., *J. Am. Chem. Soc.*, **1987**, *109*, 4184-4188.

33. Burford, N., Royan, B., Spence, R., Cameron, T., Linden, A., *J. Chem. Soc., Dalton Trans.*, **1990**, 1521-1528.

34. Dunne, B., Morris, R., Orpen, G., *J. Chem. Soc., Dalton Trans.*, **1991**, 653-664.

35. Cotton, A., Wilkinson, G., *Advanced Inorganic Chemistry*, 5th ed., John Wiley & Sons, NY, 1988.

36. Xiao, S., Trogler, W., Ellis, E., Berkovitch-Yellin, Z., *J. Am. Chem. Soc.* **1983**, *105*, 7033-7037.

37. Yang, C., Goldsteir, E., Breffle, S., Jin, S., *J. Mol. Str.*, **1992**, *259*, 3445-3468.

38. Feher. F., Budzichowski, T., Weller, K., *Polyhedron*, **1993**, *12*, 591-599.

39. Braga, M., *J. Mol. Str.*, **1992**, *253*, 167-178.

40. Ferraro, J., *Low-Frequency Vibrations of Inorganic Compounds and Coordination Compounds*, Plenum Press, NY, 1971

41. Butler, I., Harrod, J., *Inorganic Chemistry, Principles and Applications*, Benjamin/Cummings Publishing Company, Inc. NY, 1988, 618.